

Dynamics of nonmigrating mid-channel bar and superimposed dunes in a sandy-gravelly river (Loire River, France)



Coraline L. Wintenberger^a, Stéphane Rodrigues^{a,*}, Nicolas Claude^b, Philippe Jugé^c, Jean-Gabriel Bréhéret^a, Marc Villar^d

^a Université François Rabelais de Tours, E.A. 6293 GÉHCO, GéoHydrosystèmes Continentaux, Faculté des Sciences et Techniques, Parc de Grandmont, 37200 Tours, France

^b Université Paris-Est, Laboratoire d'hydraulique Saint-Venant, ENPC, EDF R&D, CETMEF, 78 400 Chatou, France

^c Université François Rabelais — Tours, CETU ELMIS, 11 quai Danton, 37 500 Chinon, France

^d INRA, UR 0588, Amélioration, Génétique et Physiologie Forestières, 2163 Avenue de la Pomme de Pin, CS 40001 Ardon, 45075 Orléans Cedex 2, France

ARTICLE INFO

Article history:

Received 11 February 2015

Received in revised form 17 July 2015

Accepted 18 July 2015

Available online 4 August 2015

Keywords:

Sandy-gravelly rivers

Nonmigrating (forced) bar

Field study

Superimposed dunes

Sediment supply

Bedforms

ABSTRACT

A field study was carried out to investigate the dynamics during floods of a nonmigrating, mid-channel bar of the Loire River (France) forced by a riffle and renewed by fluvial management works. Interactions between the bar and superimposed dunes developed from an initial flat bed were analyzed during floods using frequent mono- and multibeam echosoundings, Acoustic Doppler Profiler measurements, and sediment grain-size analysis. When water left the bar, terrestrial laser scanning and sediment sampling documented the effect of post-flood sediment reworking.

During floods a significant bar front elongation, spreading (on margins), and swelling was shown, whereas a stable area (no significant changes) was present close to the riffle. During low flows and falling limbs of floods, intense sediment reworking on the top of the bar and lateral scouring occurred. Hydrological variations controlled the sediment supply (in terms of phasing, quantity, and grain size) delivered by surrounding channels during floods and thus superimposed dune development. Their development was also linked to the sediment availability (armor layers, riffle proximity). Their relatively constant height highlights a preferential adaptation on dune length during floods.

The role of each morphological forcing parameters (riffle vs. channel widening and curvature) on the bar dynamics and evolution is stage dependent; the shape, dynamics, and long-term morphological evolution of the bar and of the river reach (surrounding islands, channel translation) mainly depends on the presence of the natural riffle.

© 2015 Elsevier B.V. All rights reserved.

1. Introduction

1.1. Background

In sandy-gravelly rivers, the development of bars is commonly observed. The height and width of these bedforms are of the same order of size as the water depth and channel width, respectively (Jackson, 1975). Bars can influence the morphological evolution of rivers through their interaction with the flow and sediment transport (Parker, 1976; Blondeaux and Seminara, 1985; Struiksma et al., 1985; Crosato and Mosselman, 2009; Hooke and Yorke, 2011; Kleinhans and Van den Berg, 2011; Eekhout et al., 2013).

In rivers, migrating bars and nonmigrating bars (corresponding to the free and forced bars of Seminara and Tubino, 1989; see review in Rodrigues et al., 2015) can be distinguished. The first type results from

the instability of turbulent flows occurring on an erodible bed and depends mainly on the aspect ratio of the channel (Callander, 1969; Colombini et al., 1987; Seminara and Tubino, 1989; Tubino, 1991). Nonmigrating bars (or forced bars) are basically stationary within the bed and develop because of changes in the channel planform or variations of the channel width (Bittner, 1994; Repetto et al., 2002; Wu and Yeh, 2005). In this case, the separation of the flow associated with an energy loss favor sediment deposition and even lateral migration of bars coming from upstream (Claude et al., 2014). Nonmigrating bars can also be induced by the presence of a steady local perturbation (riffle, groyne, and vegetation). In this case, bar deposition occurs downstream of the forcing if the width-to-depth ratio is smaller than a value of resonance and upstream if the width-to-depth ratio is larger (Zolezzi and Seminara, 2001; Zolezzi et al., 2005; Mosselman et al., 2006).

The two types of bars (migrating and nonmigrating) can coexist in river channels (Lanzoni, 2000a,b; Wu et al., 2011). Crosato et al. (2012) showed that slowly growing nonmigrating bars can develop and replace migrating bars on a long-term perspective if discharge remains constant. Contrarily, Rodrigues et al. (2015) suggested that

* Corresponding author.

E-mail address: srodrigues@univ-tours.fr (S. Rodrigues).

flow variations, specifically at low flows, can generate new migrating alternate bars.

Migrating mid-channel bars and their interactions with bed morphology have been studied extensively in the field (Leopold and Wolman, 1957; Ashworth et al., 1992; Bridge and Gabel, 1992; Richardson et al., 1996; Richardson and Thorne, 1998, 2001; McLelland et al., 1999; Reesink and Bridge, 2011) and experimentally (Ashmore, 1982, 1991; Ashworth, 1996; Federici and Paola, 2003; Reesink and Bridge, 2007, 2009). However, investigations performed on nonmigrating mid-channel bars and superimposed dunes are rare. The feedback loops that link dunes with migrating bars have been recently investigated in studies that highlighted contrasted hydrosedimentary processes according to the study context. For example, the presence of bars influences flow depth and sediment availability which will impact the development of dunes (Tuijnder et al., 2009; Claude et al., 2012, 2014). Villard and Church (2005) and Claude et al. (2012) observed on migrating bars on the Fraser River (Canada) and the Loire River (France), respectively, that the largest dunes can be found superimposed on bars suggesting that sediment supply or availability can sometimes govern dune size in a stronger way than water depth. This is in contrast with many field studies that attributed the largest dunes to reaches where water was deepest (Coleman, 1969; Thorne et al., 1993; Dalrymple and Rhodes, 1995; Ashworth et al., 2000) as reduced water depth causes a reduction in the boundary layer involved in dune development. In return, the dunes affect the bar formation and morphological evolution by modulating their vertical and lateral accretion (Bristow, 1987; Bridge, 1993; Ashworth et al., 2000; Villard and Church, 2005; Rodrigues et al., 2012, 2015).

The present study investigated the interactions between a nonmigrating bar and superimposed dunes. The bar considered is principally forced by the presence of a riffle and, in a lesser way, by an expansion area and by a low degree of curvature of the channel. Before the surveys, an initial smooth flat-bed made of a mixture of sands and gravels was ensured by fluvial management works. Surveys were performed just after works were carried out on the bar that ensured a monitoring of the bar response to the disturbance. This large data set allows us to study the bar response to the discharge fluctuation and to consider whether the development is purely stage related or also dependent on the antecedent morphology and local morphological factors.

As a general objective, this paper aims to understand and quantify the morphological evolution of a nonmigrating, mid-channel bar during flood events and after fluvial maintenance operations that ensured homogenized initial conditions in terms of topography and grain-size distribution. To reach this objective, two scientific questions are addressed.

Firstly, what is the influence of discharge variations on the dynamics of a nonmigrating bar associated with a steady perturbation (riffle) and covered by superimposed dunes during high-magnitude floods and over several flood events? More precisely, how sediment availability/supply influence bar elongation, spreading, and the development of superimposed dunes?

Secondly, how do discharge variations affect the relative weight of forcing parameters (riffle vs. expansion and curvature) responsible for a mid-channel, nonmigrating bar formation and dynamics and how, comparatively to other forced bars, do nonmigrating bars induced by a steady perturbation influence the morphological evolution of a river reach?

1.2. Loire River and study site

1.2.1. The Loire River

The Loire River is 1012 km² in length and drains a catchment area of 117,000 km² in France. At Orleans (638 km from the source), the river flows through sedimentary rocks of the Paris basin and shows a range of fluvial patterns from single channel (straight or meandering) to

anabranching. For bankfull discharge rates, the width-to-depth ratio ranges between 50 and 150 (Latapie et al., 2014). Two climatic influences determine the regime of the Loire: rainfall coming from the Atlantic Ocean (mainly during winter) or rain storms in the upper mountainous reaches that occur during spring (Dacharry, 1996).

A severe incision of the main branch of the river, owing to a combined effect of the groynes for navigation (nineteenth to twentieth centuries) and intense sediment extraction (1950–1995), led to exposure of the bedrock, affecting the slope and thus the morphology of the Loire River. Bank erosion and lateral shifting is also constrained by artificial levees built for flood prevention (Latapie, 2011).

As a consequence, associated with a decrease in flooding, side channels and alluvial bars were rapidly colonized by woody vegetation that enhances sediment deposition (Rodrigues et al., 2006, 2007) and reduces habitat diversity and flow capacity during floods.

1.2.2. Study site

The study site of Mareau-aux-Prés (Fig. 1) is located about 10 km downstream of Orleans (649 km from the source), downstream of the confluence with the Loiret River that is a resurgence of the Loire River. At the Orleans gauging station, the average discharge of the Loire is 344 m³ s⁻¹ and its 2-year flood discharge is 1700 m³ s⁻¹.

At Mareau-aux-Prés, the anabranching fluvial pattern is characterized by a set of islands present for several decades (Fig. 1). This reach is characterized by a contraction–expansion area with a channel width varying from 270 to 430 m between artificial levees preventing lateral erosion and lateral sediment supply. On the right bank, an artificial curvature deflects the main channel course toward the southwest, while a side channel flows straight near the left bank. This river reach has a sinuosity index of 1.04 and an average slope of 0.00023 m m⁻¹ (Latapie, 2011). The water surface is locally modified caused by two natural bedrock riffles (Fig. 1) and a nonmigrating mid-channel bar consisting of siliceous sands, gravels, and pebbles that developed between these two riffles. This bar constitutes the central part of an asymmetrical bifurcation splitting two channels of different sizes (main and secondary channels; Fig. 1) as commonly shown in the literature (Miori et al., 2006; Zolezzi et al., 2006). During floods, flow coming from the main channel is divided by the small island 1 (Fig. 1B). The mid-channel bar was colonized by pioneer trees (*Salicaceae*) in 2005 and evolved rapidly as an island until 2012 (Wintenberger et al., 2015). In September 2012, fluvial management works (FMW) were carried out. They consisted of cutting down the vegetation, extracting the root systems, and lowering the average elevation of the island by exporting the bar sediments into the main channel. After this work, the alluvial bar was characterized by a flat surface of 26,700 m²; no bedforms were present anymore, except for some small ridges and swales mostly oriented in the flow direction. Sediments were homogenized on the bar to a depth of 0.5 m, disturbing the initial spatial organization of grain size. Following the management works, the bar was submerged at a discharge value of 300 m³ s⁻¹ (Orléans gauging station, 10 km upstream).

2. Material and methods

During low flow stages and flood periods, data were collected to characterize the hydrodynamic, morphological evolutions, and the sedimentary conditions over the mid-channel bar. Before the submersion of the bar (October 2012), the topography was acquired and sediments were sampled as presented in Fig. 1. During the flood period from December 2012 to June 2013, 17 field surveys (from S1 to S17) were carried out for discharge values ranging from 400 to 1900 m³ s⁻¹ (Fig. 2). The discharge was given at the gauging station of Orléans by the DREAL Centre (environmental agency). These 17 surveys always consisted of a bathymetric survey in addition with flow velocity for 13 surveys (S1, S2, S3, and S9 excluded because of field conditions) and sediment sampling for six surveys (S10, S13, S14, S15, S16, and S17; see Figs. 2 and 10). At the emersion of the bar in June 2013, topography

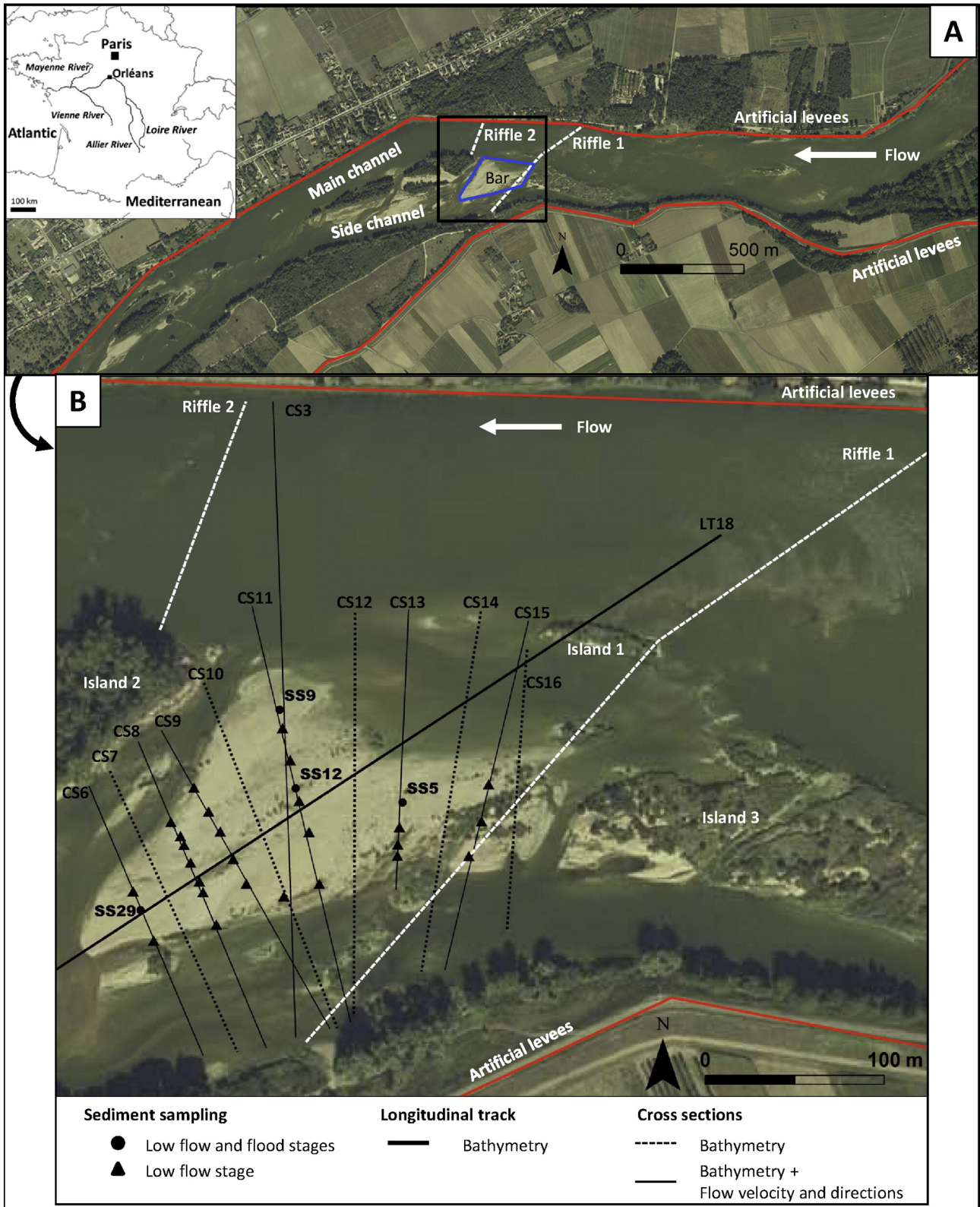


Fig. 1. Study site of Mareau-aux-Prés, located in the middle reaches of the Loire River (aerial photographs from DREAL Centre) and 10 km downstream of the city of Orléans. (A) The morphological context in a contraction–expansion area associated with channel curvature and natural riffles because of the bedrock exposure of where the nonmigrating, mid-channel bar developed. (B) Cross sections and longitudinal track followed by bathymetric and hydraulic surveys associated with sediment sampling.

measurements were performed again together with sediment sampling. All the data were georeferenced using a dGPS system (real time kinematic, differential centimetrical corrections) referenced in the French national system (Lambert 93).

The methodology applied in this study is similar to the approach detailed in [Claude et al. \(2012\)](#). The reader is invited to refer to this publication for more details. Average parameters of hydraulic conditions on the bar during surveys are available in [Table 1](#) (see the [Results](#) section).

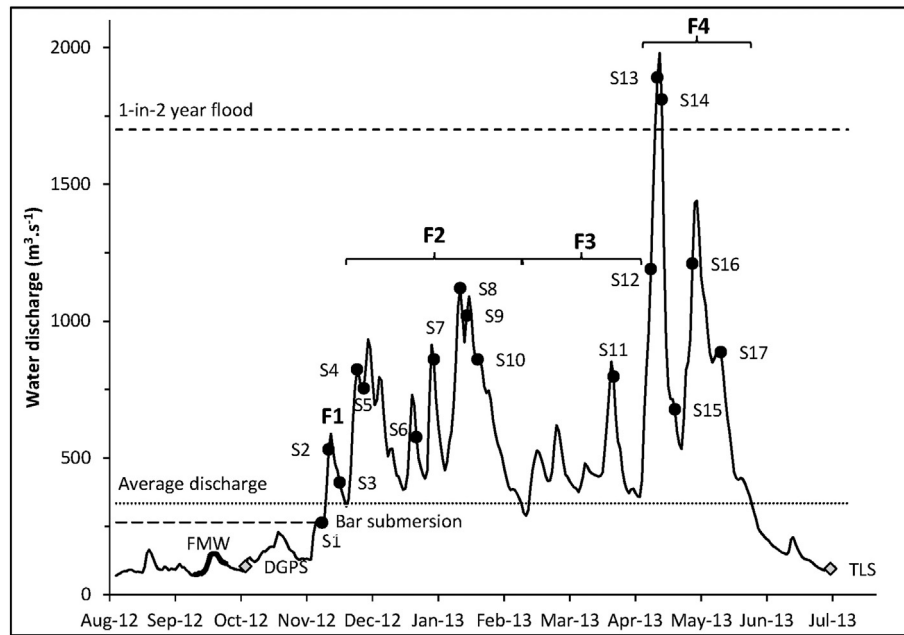


Fig. 2. Four floods occurred during the study period (F1, F2, F3, and F4). For each flood one to four surveys were done to document rising, peaks and falling stages. The fluvial management works (FMW) were done during low-flow conditions. Gray diamonds refer to the topographic surveys (DGPS and TLS). Black circles refer to the bathymetric surveys associated with flow velocity measurements and sediment sampling (SS).

2.1. Hydraulics

Flow velocities were acquired using an M9 ADP (Sontek), which has two sets of four profiling beams (at 3 and at 1 MHz), and connected to a differential global positioning system (dGPS) Magellan ProFlex 500 over seven cross sections (Fig. 1B). During each survey, the flow velocities on cross sections were measured four times at a boat speed of about 1 m s^{-1} . The flow velocities recorded on each cross section were projected on a grid with cells 3 m wide and a height equal to the maximum height of the bins defined during the measurements (Dinehart and Burau, 2005a,b). The flow velocities (estimated in each bin) were then averaged in each 3-m-wide cell to obtain one value per cell. Finally, the flow velocities and water depths were averaged for each vertical line to obtain the mean flow velocity. The bottom velocity corresponds to a cell located near the bed. This method was also applied by Claude et al. (2014) and more details are available in this paper.

The bed shear stress was calculated in relation to the flow velocity profile and the law of the wall (Sime et al., 2007) over the bar area using the following equation:

$$\tau = \rho \left[\frac{ku}{\ln\left(\frac{z}{(z_0)_{SF}}\right)} \right]^2 \quad (3)$$

where u is the flow velocity at height z over the bed, k is the von Karman constant equal to 0.4 for clear waters, and $(z_0)_{SF}$ is the grain roughness (or the height at which $u = 0$) equal to $0.095 D_{90}$ (Wilcock, 1996). The adjustment made by linear regression between the values of u and $\ln(z)$ measured on a vertical line allows the calculation of τ (Sime et al., 2007; Szupiany et al., 2007, 2009; Rennie and Church, 2010).

The averaged flow velocities for each vertical and bed shear stress associated, derived from the law of the wall, allowed us to calculate a mean value for each cross section for each survey. Then, the mean values by cross sections were used to calculate the mean flow velocity and the mean bed shear stress (Table 1).

2.2. Bed morphology and sediment transport

When the bar emerged, topographic surveys were conducted (Fig. 1). In October 2012, topographic measurements were done using the dGPS Magellan ProFlex 500 (Fig. 2). An average of 6 points/m² was recorded to provide an appropriate representation of the slope breaks on the bar. The Triangular Interpolation Network (TIN) tool of ArcGIS10 software was used to obtain digital elevation models (DEMs) with a 1-m mesh. In June 2013, a terrestrial laser scanner (TLS) survey was done (800 points/m²) (Fig. 2). The TLS Leica HDS 3000 station driven by the Cyclone 7.3 software (Leica Geosystems) was used, and DEMs were obtained using the above-mentioned method (TIN). Four targets were set up around the station, located on perennial bench marks (50-cm long metal tubes with plastic heads) georeferenced using the dGPS during the TLS survey. During floods with lower discharges than the flood with a 2-year return period (Fig. 2), bathymetric surveys were performed using a monobeam echo-sounder (Tritech PA500 – 500 kHz) over 12 cross sections (Fig. 1) and one longitudinal track (LT18). The longitudinal track was surveyed twice during a single survey (<1 h between two crossings) allowing the calculation of dune celerity (Simons et al., 1965; Peters and Sterling, 1975; Peters, 1978). For discharge values higher than the flood with a 2-year return period (Fig. 2), bathymetric surveys were performed using an Odom ES3 multibeam echo-sounder with 240 beams (240 kHz with 120° opening). The two echo-sounders were connected to a dGPS Magellan ProFlex 500 and driven by Hypack 2009 software. Accuracy of the measurements was 0.1 m during navigation and densities of points ranged from 0.2 to 0.6 points/m² for the monobeam surveys and 2 points/m² for the multibeam surveys. Bathymetric cross sections were compared using Hypack 2009 and ArcGIS 10 software. The transversal scour-and-fill areas between each survey were quantified in terms of sediment budget using the Average End Area 3 function of Hypack 2009 (Rodrigues et al., 2012). The errors were estimated combining the total length of sections to the accuracy of measurements and the results ranged between 9 and 15 m³. The longitudinal integration of these budgets over the nonmigrating bar documented the dynamics of the bedload sediment supply delivered by the main channel. The dune

Table 1
Average hydraulic and sediment transport parameters for each survey on the bar^a.

Flood	Flood stage	Survey number	Discharge (m ³ s ⁻¹)	Average water depth (m)	Mean flow velocity (m s ⁻¹)	Average bed shear stress (N m ⁻²)	Number of dunes	Dune celerity (m s ⁻¹)	qb _{DTM} (kg s ⁻¹ m ⁻¹)
F1	Rise	S1	0264	<0.7	No data	No data	No data	No data	No data
	Rise	S2	0527	No data	No data	No data	24	45.10 ⁻⁵	0.05–0.07
	Fall	S3	0400	No data	No data	No data	22	44.10 ⁻⁵	0.07–0.1
F2	Peak	S4	0790	<1.43	1.2	4.8	50	50.10 ⁻⁵	0.08–0.12
	Fall	S5	0729	<1.22	1.1	2.1	46	43.10 ⁻⁵	0.09–0.12
	Fall	S6	0576	<0.9	0.9	2.7	28	24.10 ⁻⁵	0.04–0.06
	Fall	S7	0860	<1.19	1.1	5.3	66	43.10 ⁻⁵	0.08–0.11
	Peak	S8	1120	<1.55	1.1	5.7	30	48.10 ⁻⁵	0.10–0.14
	Rising	S9	1020	No data	No data	No data	36	65.10 ⁻⁵	0.13–0.18
	Fall	S10	0860	<1.28	1	4.2	38	39.10 ⁻⁵	0.08–0.11
F3	Fall	S11	0797	<1.21	1	4.2	34	42.10 ⁻⁵	0.06–0.08
F4	Rise	S12	1190	<1.81	1.4	6.6	No data	No data	No data
	Rise	S13	1890	<2.79	1.6	12	No data	No data	No data
	Fall	S14	1810	<2.43	1.6	7.6	06	80.10 ⁻⁵	0.16–0.23
	Fall	S15	0677	<0.92	1	2.6	No data	No data	No data
	Rise	S16	1210	<1.7	1.3	4.3	56	60.10 ⁻⁵	0.10–0.15
	Fall	S17	0886	<1.13	1.1	5.3	26	76.10 ⁻⁵	0.15–0.21

^a The water depth is the depth in the intersection between the LT18 and the CS3. For survey S1, navigation was impossible because of insufficient flow depth. Discharge values were provided by the DREAL Centre (environmental agency) for the Orleans gauging station (10 km upstream).

heights (H_d) and lengths (L_d) were determined using the Matlab code bedform tracking tool (BTT), based on a zero-crossing method (Van der Mark et al., 2007, 2008). This method was applied on a part of

LT18 (160–300 m), surveyed during floods lower than the flood with a 2-year return period, delimited downstream by the front of the bar (which could distort the adjustment of the trend line) and by the

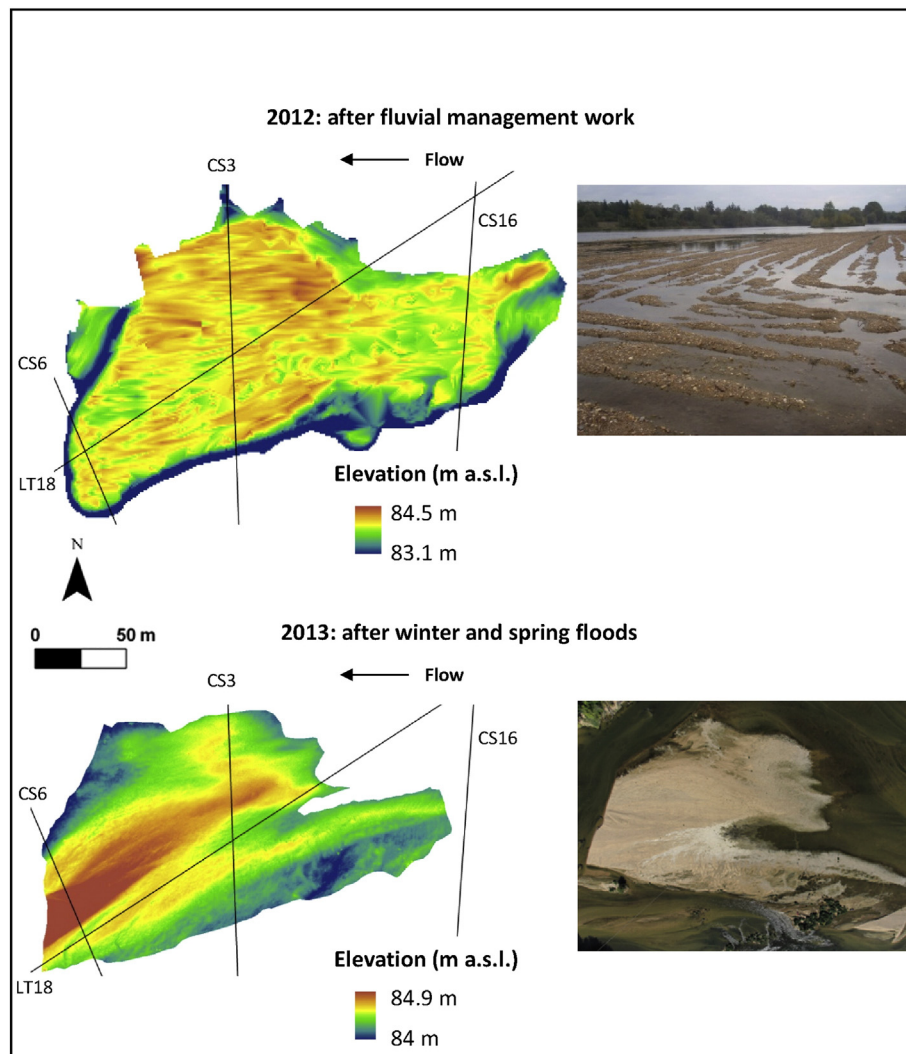


Fig. 3. Digital elevation models (DEM) after fluvial management works with ground picture oriented downstream illustrating the ridge-and-swale topography (2012) and after floods of 2013 (aerial picture, smooth topography).

upstream limit of dune development. Using the BTT results, evolution of the dune shape was studied using the steepness value defined as the ratio between dune height and length.

The bedload transport rate related to bedform migration (Simons et al., 1965; Van Den Berg, 1987; Kostaschuk et al., 1989; Ten Brinke et al., 1999; Hoekstra et al., 2004; Gaeuman and Jacobson, 2007) was calculated using the classical equation of the dune tracking method:

$$qb_{DTM} = \rho_s \varepsilon \beta c_D H_D \quad (2)$$

where qb_{DTM} is the unit bedload ($\text{kg} \cdot \text{s}^{-1} \cdot \text{m}^{-1}$); c_D is the dune celerity ($\text{m} \cdot \text{s}^{-1}$); H_D is the dune height (m); ε porosity of sediment; ρ_s density of sediment; and β is the bedload discharge coefficient taking into account the deviation of the bedform shape (Gaeuman and Jacobson, 2007). This coefficient varies between 0.46 and 0.66 (Van Den Berg, 1987; Villard and Church, 2003; Hoekstra et al., 2004; Pinto Martins et al., 2009). On the middle reaches of the Loire, it ranges between 0.46 and 0.56 (Claude et al., 2012).

2.3. Grain-size analyses

A total of 30 plots (Fig. 1B) of surface bed sediments located using the dGPS were sampled for grain-size analysis immediately after the fluvial management works and one year later during low flows. When armored layers were present, the surface and sublayer sediments were sampled independently. During floods, four of these plots were surveyed using a grab (Fig. 1B).

Sediment samples were analyzed by dry sieving using a vibratory sieve shaker (Retsch 3D – AS450). The fraction finer than $63 \mu\text{m}$ (negligible in the river bed of the Loire; Macaire et al., 2013) was excluded. The classical grain-size parameters were obtained using the Gradistat

4.0 spreadsheet (Blott and Pye, 2001) with the arithmetic Folk and Ward method.

3. Results

Table 1 contains average hydraulic and sediment transport parameters as a function of the stage of flood for each survey.

3.1. Hydrological history

After the fluvial management works (2012), four subsequent winter and spring floods occurred. In this paper, a flood is defined as the hydrologic variations higher than the average discharge. These flood events were responsible for the morphological evolution of the bar after the management works. The ridge-and-swale morphology was replaced by bedforms for which elevation varied between 84 and 84.9 m (Fig. 3). The flood F1 is a single-peak flood, whereas the others are multiple-peak floods. During F1 and F4, rising, falling limbs, and peak discharges were captured respectively with three (S1, S2, and S3) and six (S12, S13, S14, S15, S16, and S17) surveys. Floods F2 and F3 were respectively described with seven (S4, S5, S6, S7, S8, S9, and S10) and one (S11) surveys excluding the rising limb. The maximum discharge of the F3 flood is comparable with the discharge of the winter floods. The flood F4 exceeds the value of a flood with a 2-year return period. The effect of the highest peak discharge (F4) was detailed using two surveys performed during the rising stage (middle and end) and two surveys done during the falling stage (beginning and end).

During floods, the water depth increases with the discharge for the range of 576 to $1810 \text{ m}^3 \cdot \text{s}^{-1}$. So the water depth depends mainly on the fluctuations of discharge. However, the vertical deformation of the nonmigrating bar during floods occasionally disturbs this trend.

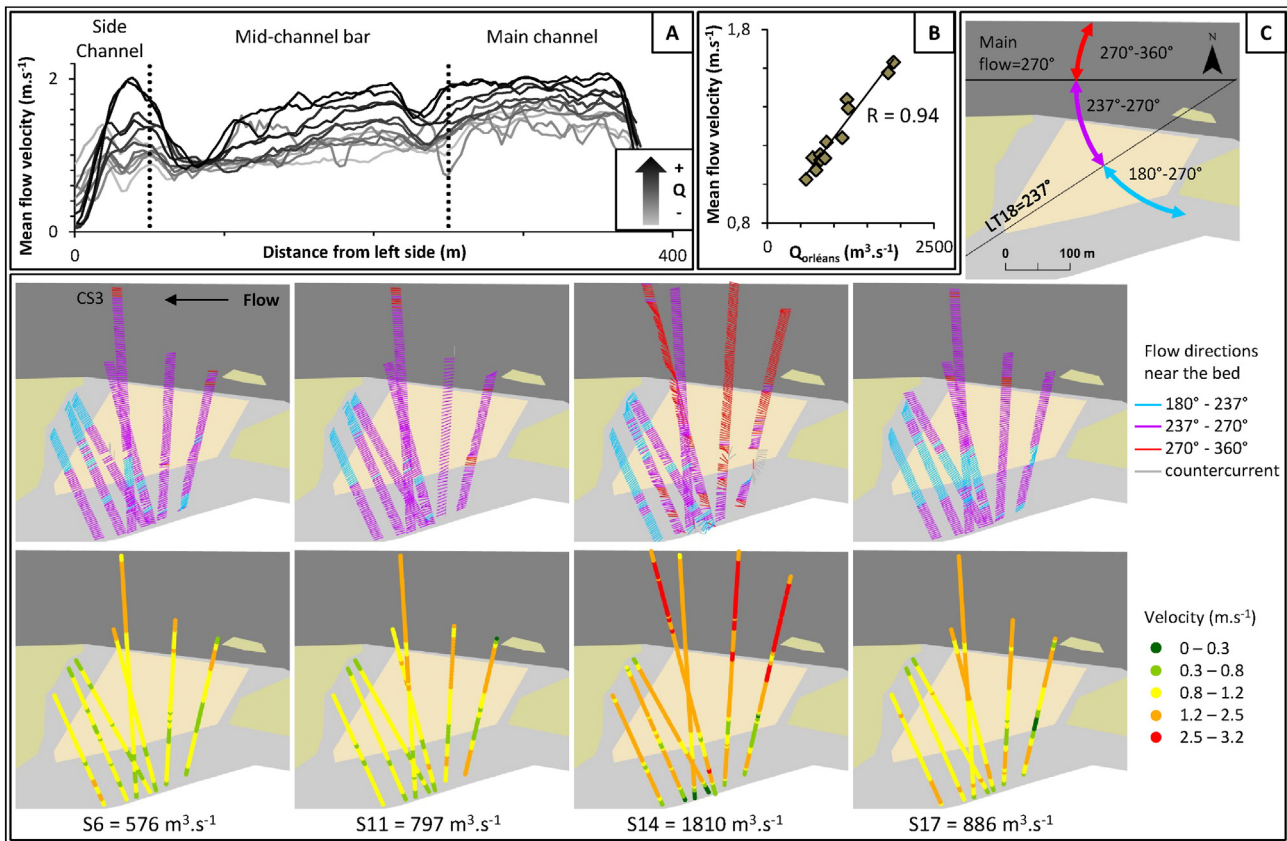


Fig. 4. Mean flow velocities along the cross section CS3 (see location on this figure, C) with darker curves for high flows and pale gray for the lower (A). The mean flow velocities measured on the bar are averaged and compared to water discharge on the cross section CS3 (B). Mean directions and flow velocities measured on all cross sections for height surveys and associated bed shear stress (C). Directions are classified according to their deviation from the direction of the longitudinal track LT18 (237°) and the main flow (270°).

3.2. Effects of discharge conditions on flow velocity and bed shear stress

On the bar, mean daily flow velocities varied between 0.9 and 1.6 m s⁻¹. Globally, the flow velocities decrease from the main channel to the left side and from upstream to downstream. The spatial distribution is determined by the site morphology, but this influence decreases as the discharge increases. The mean flow velocity and the flow velocity near the bed follow the same trend: increasing with discharge (Fig. 4B). In the upstream part of the bar, established islands and riffles create lee areas with low flow velocities and narrow channels with high flow velocities. For high discharge values (1810 m³ s⁻¹, survey S14), flow velocities are high and show a more homogeneous distribution over the bar compared with lower discharges. Associated bed shear stress calculated range from 0 to 20 N m⁻²; mean and median values equal to 4.6

and 3.3 N m⁻², respectively. The shear stress is higher in the upstream part of the bar than downstream.

On the bar, the flow directions are oriented southwest (between 270° [main channel direction] and 237° [LT18 direction]) owing to the deflection of the channel curvature. The flow on the downstream part of the bar is deflected toward the side channel caused by the presence of the downstream island and the riffle. However, during high discharges, the deflection effect decreases in the upstream part of the bar and flow directions are oriented toward the concave bank of the main channel (Fig. 4C, S14). For low discharges occurring during the falling stage, the flow directions oriented toward the side channel appear close to the middle part of the bar (Fig. 4C, S17). At this stage, the elevation of water in the main channel is higher than in the side channel, intensifying the deflection effect.

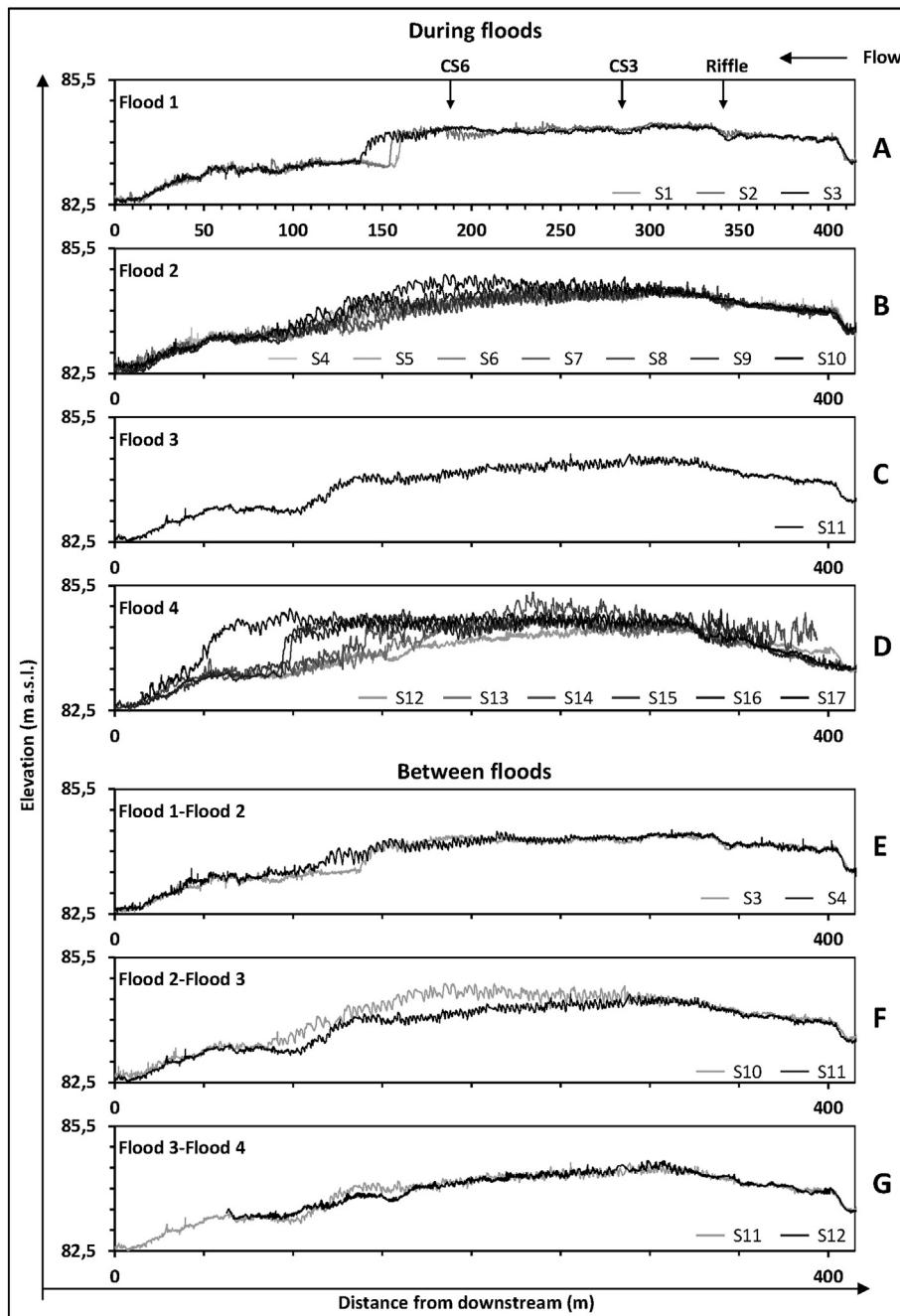


Fig. 5. Longitudinal bathymetrical (LT18) evolution of the bar during floods (A, B, C, D) and between floods (E, F, G) with darker curves for more recent surveys and pale gray for older surveys.

3.3. Effects of discharge variation on bar morphology

During the rising stage of the first flood, the front and the back of the bar are stable (Fig. 5A). At the falling stage, the bar front spreads 15 m downstream but the back of the bar is not modified (Fig. 5A). During flood F2, the bar-top becomes convex, while the front slope decreases (Fig. 5B). The front and the upstream part of the bar are stable, reflecting sediment storage. During flood 3, the bar-top recovers a flat surface and a high slope of the front bar (Fig. 5C). During the last flood F4, and for the first time, the bar becomes convex again (Fig. 5D). Since the first falling stage, the bar-top becomes flat with a well-developed front that spreads downstream over a hundred meters. In contrast with the previous morphologies, this resulting flat morphology is set up at a high topographic

elevation. Between the first and last surveys of two consecutive floods, flood 1–flood 2 (Fig. 5E) and flood 3–flood 4 (Fig. 5G), the inherited morphology of the previous flood is preserved at the beginning of the rising stage of the following flood. The evolutions are very small; only the bar front reveals a spread of a few meters. In contrast, the inherited morphology at the end of flood 2 is convex (Fig. 5F). The lower topography surveyed during flood 3 shows erosion between the two consecutive floods separated by a falling stage driving to the emersion of the bar.

The 84.2-m isoline was defined as representative of the contour of the bar and is used to determine the evolution of the bar planform during flood events (Fig. 6). The total surface area over which the bar evolves is 38,000 m²; the position of bar edges fluctuates downstream and laterally over an area of 29,000 m² around a fixed area of 9000 m²

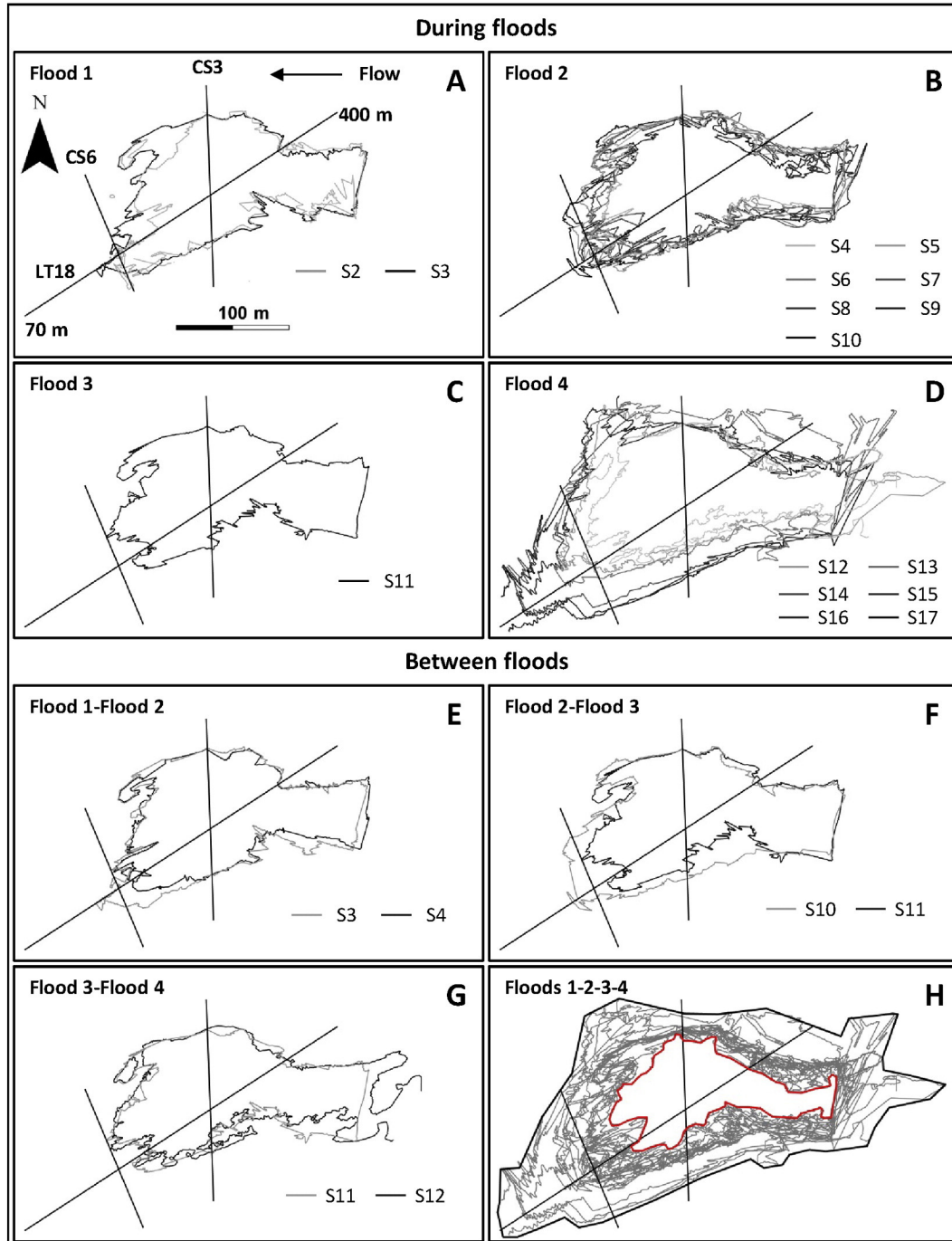


Fig. 6. Bar edges, characterized by the isoline 84.2 m, evolution during floods (A, B, C, D) and between successive floods (E, F, G, H). Distances on the LT18 refer to distance from downstream in Fig. 5.

(Fig. 6H). During flood 1, the elongation observed on the longitudinal track (Fig. 5A) is limited to the right side of the front of the bar (Fig. 6A). Bar edges located upstream of cross section CS3 and south of LT18 are stable. During flood 2, lateral edges vary with an elongation of the bar front (Fig. 6B) but no significant lateral spreading occurred. As observed on the longitudinal track, the front elongates during flood 4 in a first stage only in the downstream direction. In a second stage, the bar spreads toward the side channel in the south. During the flood, the downstream elongation velocities range from 0.5 to 5 m d⁻¹. The upstream part is more stable with nonregular lines in

the riffle location. The bar edge evolutions between successive floods (Fig. 6E,F,G) confirm the trend observed on the longitudinal track (Fig. 5E,F,G). There are low variations between flood1–flood 2 (Fig. 6E) and flood 3–flood 4 (Fig. 6G). However, front erosion is revealed on the left side that does not appear on the longitudinal track. Between flood 2 and flood 3, erosion is observed on the entire front of the bar and on the south bar edges located close to the side channel (Fig. 6F). During the study, the location of the front varied by 100 m, the left-bank by 50 m, and the upstream limit by 25 m during floods (Figs. 5 and 6).

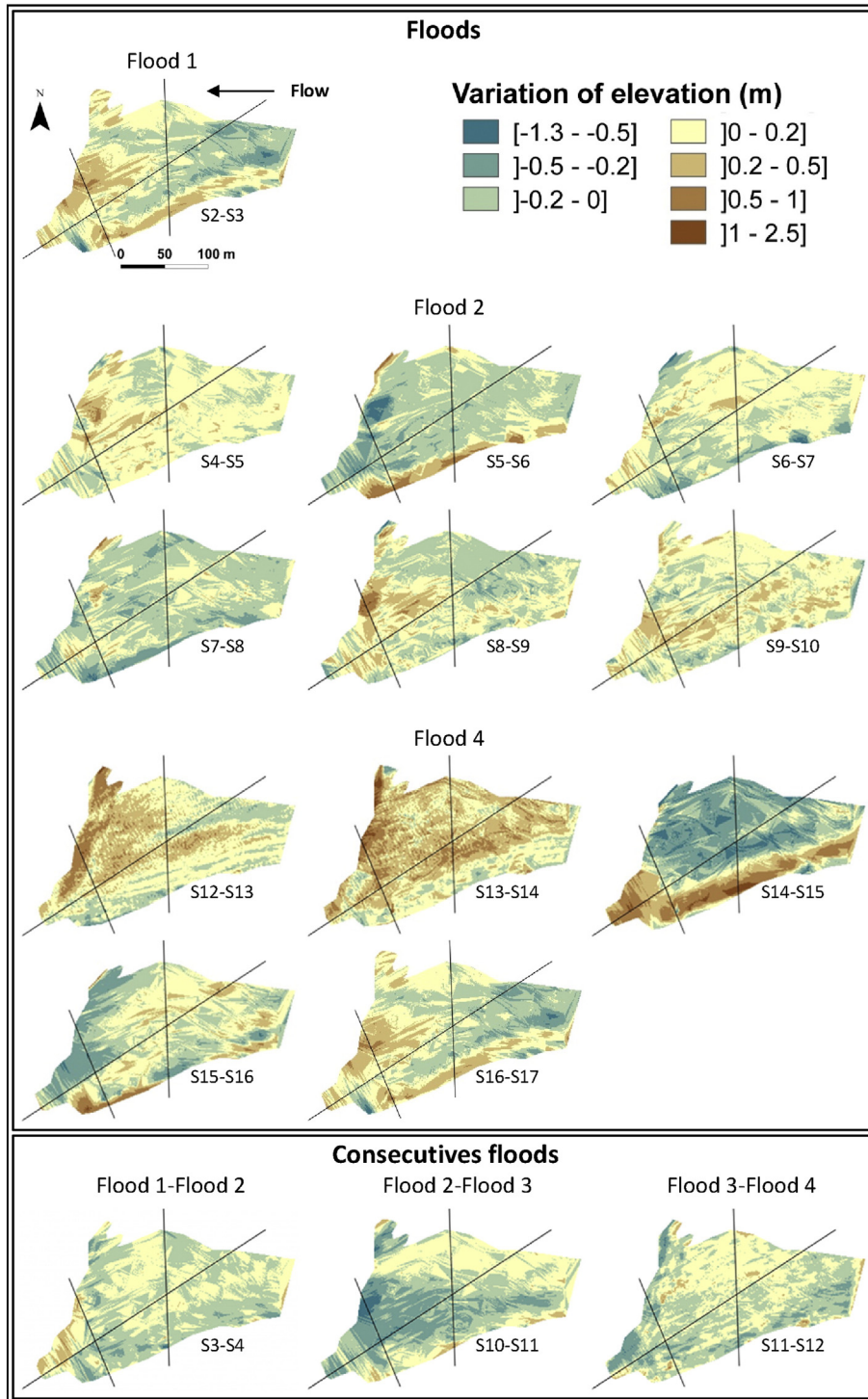


Fig. 7. Elevation variations between two successive surveys during floods for floods 1, 2, and 4 and between successive floods between the four floods. The maps are ordered chronologically of the successive surveys.

The deposition heights vary from a few centimeters to more than 2 m (Fig. 7). The variations of elevation are more important during flood 4 than the floods of lower discharges. Over the study, deposition of 0.5 to 2.5 m is observed in the front area and on the bar edges (left side). In contrast, the erosion heights rarely exceed 0.5 m. The stronger erosion appeared between flood 2 and flood 3.

Deposition on the bar-top and bar front is correlated with sediment supply from the main channel. The stability of the upstream part of the longitudinal track (Fig. 6) and the absence of marked erosion on elevation maps (Fig. 7) or on cross-sectional sediment budget curves (Fig. 8) suggest a supply from the main channel. At the beginning of sediment supply occurring during floods, sediments are coming laterally from the main channel, as highlighted by the increase of the downstream cross-sectional volumes (Fig. 8A and C). In a second time, sediments come from upstream (Fig. 8B and D). For low discharges, the lateral supply is delivered at the beginning of the falling limb and then followed by the upstream supply. In contrast, for high discharges, the lateral supply occurs during the rising stage and the upstream supply since the beginning of the falling stage. During time intervals flood 1–flood 2 and flood 3–flood 4, volumes of eroded and deposited material have the same order of magnitude (Fig. 8E and G). Between flood 2 and flood 3, volumes of erosion are important and grow downstream (Fig. 8F).

3.4. Sediment grain size

During the engineering works of 2012, sediments were mixed and no previously existing sedimentary structures remained. Two sediment populations can be distinguished (Fig. 9A) and were still present in 2013. Sediments of the first group are finer and better sorted. The two populations are finer in 2012 than in 2013. In 2012, the mean grain size corresponds in majority to coarse sands, whereas in 2013 only for sediments of the first group. Sediments of the second group have mean grain sizes corresponding to the gravel class. While sediments in 2013 are coarser, four sediment samples on the middle part of the bar have finer grain sizes and switched from group 2 to group 1 (Fig. 9B). Two sediment samples on bar edges have an opposite trend that highlights a reorganization of the sediments on the bar (Fig. 9B) leading to a fining distribution from upstream to downstream.

During the first peak of flood 4 (S13, S14, and S15), sediments SS5 (Fig. 10A) and SS9 (Fig. 10B) become finer after the peak, whereas sediments SS12 (Fig. 10C) and SS29 (Fig. 10D) become coarser. During the second peak of flood 4 (S16 and S17), sediments SS12 and SS5 become finer during the falling stage, whereas sediments SS9 and SS29 become coarser. On the SS9 location, the falling stage promotes armor layer development with a grain-size mixture similar to the sediments of 2012. Sandy sediments correspond to particles supplied

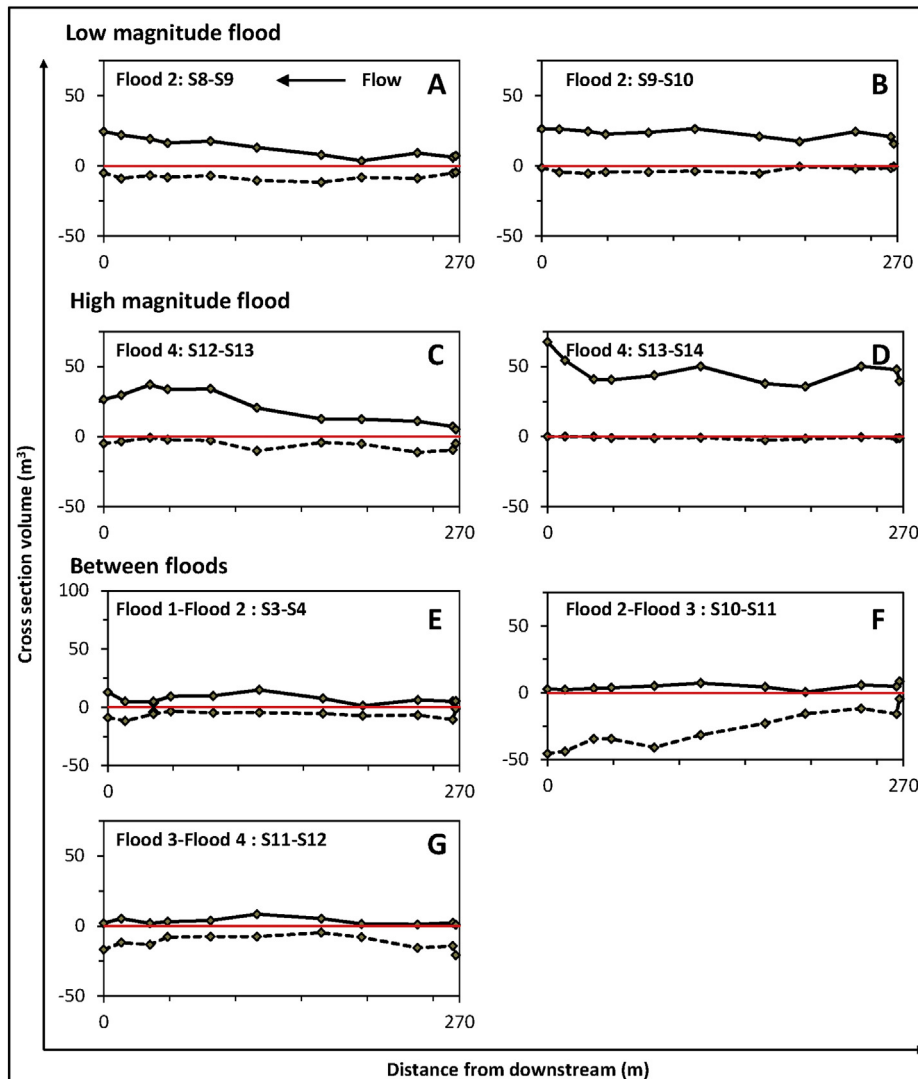


Fig. 8. Sediment budget calculated between two successive surveys on each cross section with an error estimated between 9 and 15 m³. Gray diamonds refer to the cross section locations, from CS16 (270 m upstream) to CS6 (0 m).

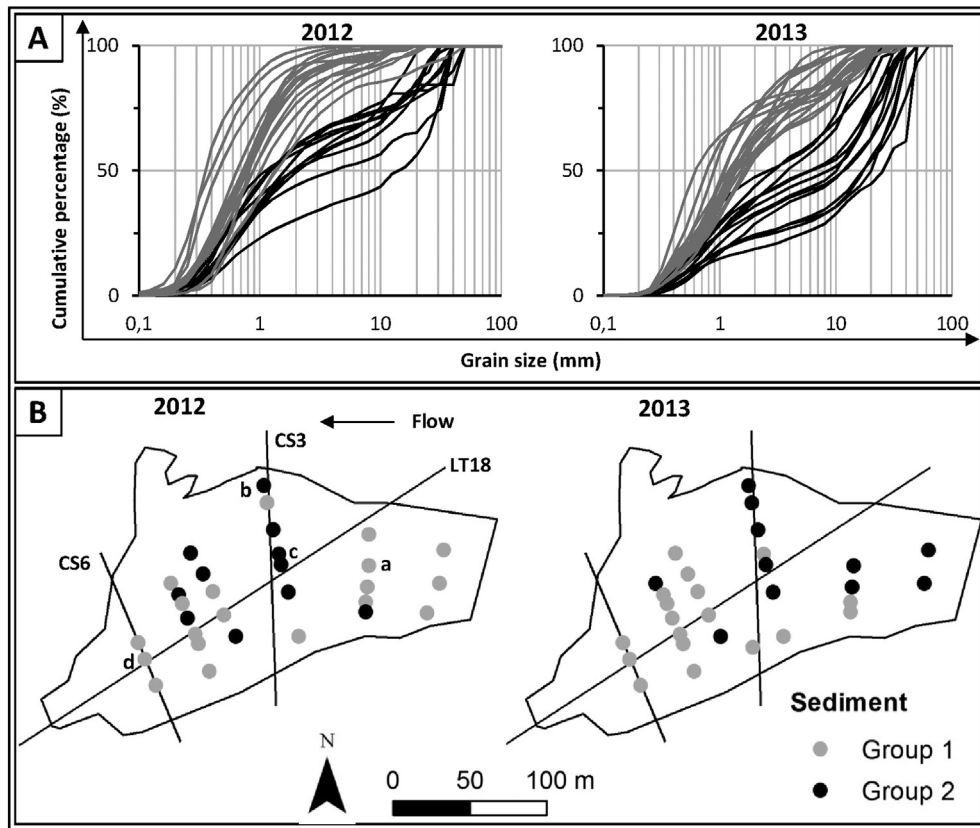


Fig. 9. (A) Grain size of sediments sampled on the bar (gray cumulative curves for group 1, black lines for group 2) in 2012 and 2013. (B) Spatial distribution of sediments on the bar in 2012 and 2013. The letters A, B, C, and D refer to the location of sediment sampling during floods SS5, SS9, SS12 and SS29 (respectively).

by the main channel during floods (and highlighted in the bathymetrical surveys). In 2013, armor layers developed on the SS9 and SS5 locations. However, SS5 shows a lag time in armor layer development during the falling stage and fining during the rising stage. Sediment grain size depends on lateral sediment supply on SS29 and SS9 and on the upstream supply on SS5 and SS12.

The relationship between the calculated bed shear stress and the D_{50} of sediments sampled during floods was integrated into the Southard and Boguchwal (1990)'s diagram (Fig. 11). For low discharges, the bed shear stress was sometimes insufficient to induce sediment motion (I on Fig. 11). According to the diagram, hydraulic conditions can favor a transition between the dune and the upper stage plane bed during the highest discharge conditions when high flow strength induces a larger portion of bed material to be transported as suspended material (Bridge and Best, 1988; Naqshband, 2014). The result can be an increase in suspended load to the detriment of bedload and so should affect dune geometry. For all the surveys, conditions are favorable for dune development on the back of the bar, specifically for SS12 and SS29 sediment sampling located on the longitudinal track (LT18) and SS5 located upstream. Sediments sampled in SS9 present less favorable conditions for dune development.

3.5. Superimposed dune morphology and dynamics

3.5.1. Geometry

Only one population of dunes migrates on the bar during each survey (Fig. 12A). The number of dunes identified for each survey is given in Table 1. The majority of surveys (12 out of 16) shows a representative dune height of 0.2 m associated with three wavelength classes: (i) 0.5–1 m (group 1); (ii) 1.5–2 m (group 2); and (iii) 2–2.5 m (group 3) (Fig. 12A). Dunes in the other surveys have heights and lengths of 0.2–0.3 m and 3–3.5 m, respectively (group 4) (Fig. 12A).

Dunes observed during the high discharges of flood 4 (S14) have a straight crest reminiscent of two-dimensional dunes (Fig. 12B).

On the bar, medium dunes ($1\text{ m} < L < 10\text{ m}$) are located between the two curves established by Flemming (1988) and Ashley (1990) (Fig. 13A). In contrast, small dunes ($L < 1\text{ m}$) are frequently higher than the maximum height calculated by Ashley (1990) (Fig. 13A). The median dune heights and lengths are in line with the theoretical values except during the two highest discharges surveyed. More than half of the dunes have steepness values between 0.06 and 0.12 (Fig. 12C). The steepness values are high for the dunes of metric-order lengths. Once their lengths are plurimetric, their steepness becomes markedly lower, as was observed on the Rhine by Carling et al. (2000) (Fig. 13B).

During the monitored flood events, water depth on the mid-channel bar varied between 0.9 and 2.8 m. The dune heights are in agreement with the maximum equilibrium height of river dunes (Kleinhans et al., 2002; Fig. 14A). For half of the surveys, heights are close to the maximum equilibrium height for which water depth is the limiting factor (Fig. 14A). However, for the other surveys, dune heights remain small and lower than maximum equilibrium height of river dunes even for the deepest water conditions (Fig. 14A). These results contrast with the primary factor of control on dune morphology assumed to be the water depth in the case of depth-limiting conditions (Flemming, 2000). However, dune heights are comparable to the predictive model by Allen (1968) (Fig. 15B) as also shown on the Fraser River by Kostaschuk and Best (2005). Dune lengths are also well predicted except for three successive surveys (S12, S13, and S14) conducted during the high-magnitude flood associated with deepest water and following strong erosion during emersion of the bar.

The adaptation of the dunes to hydrological variations reveals an anticlockwise hysteresis for the high-magnitude flood (Fig. 15). However, the evolution of length and height parameters does not systematically follow the same trend, and the lag time for these two parameters to

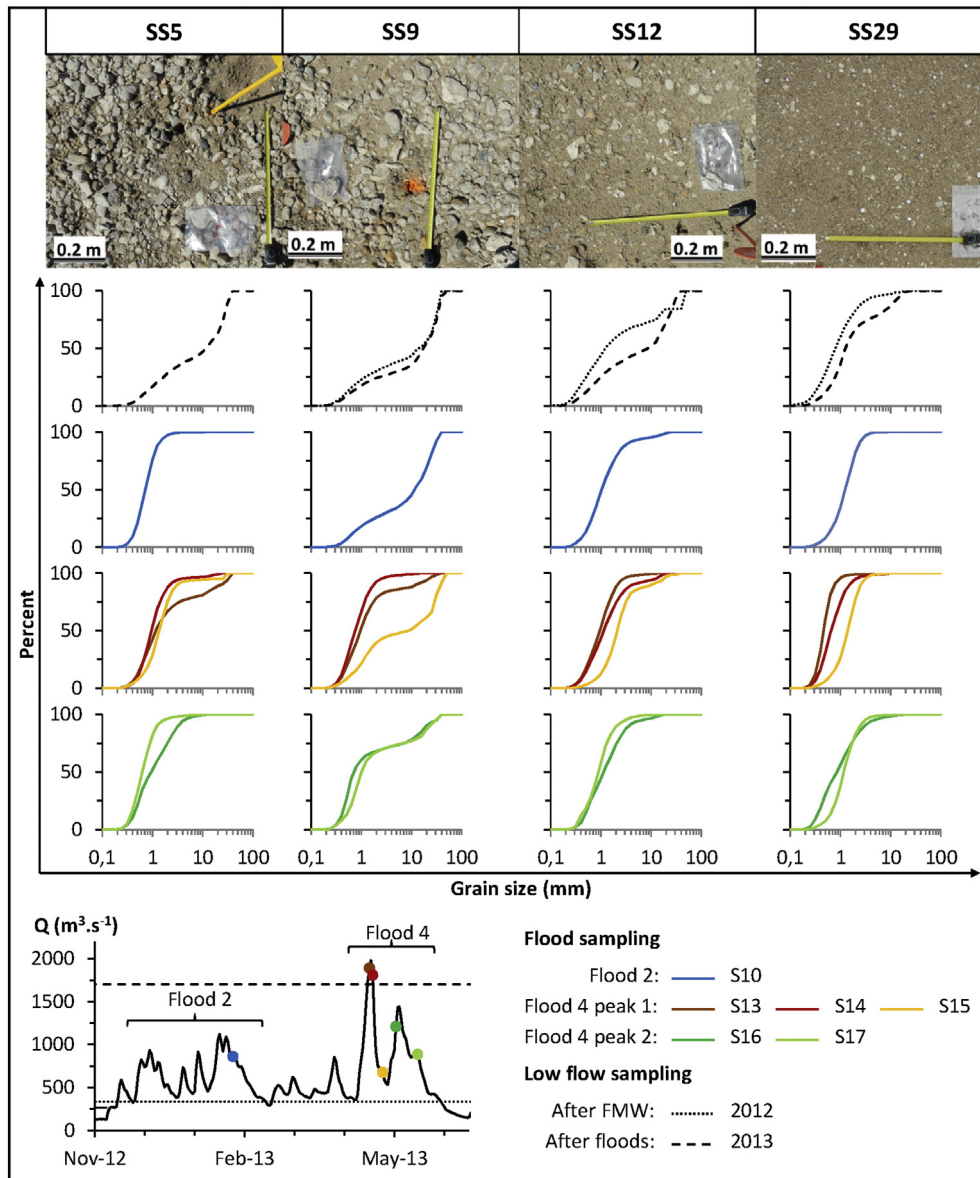


Fig. 10. Pictures show sediment surface in 2013 at four sampling sites (SS5, 9, 12, and 29). Cumulative curves refer to grain-size evolution between 2012 and 2013 (black dashed curves) and during floods 2 and 4. The color of curves refers to sampling dates presented on the hydrograph.

adjust differed. Unfortunately, because of the slight variation in dune height relative to the accuracy of measurements, it is difficult to clearly conclude on this point.

On migrating bars, sediment availability can promote dune growth, the influence of water depth becoming, in this case, secondary (Villard and Church, 2005; Claude et al., 2012). On the nonmigrating bar studied, although deep water depth occurred during floods, dune height remained low even if hydraulics and grain-size conditions were favorable to dune development. This suggests that sediment supply becomes the major limiting factor. The low erosion observed during floods (Fig. 8) suggests that sediment stored on the nonmigrating bar only slightly feeds the dunes. They grow once the sediment supply is provided by the main channel (after the peak discharge) and according to a lag time of adaptation.

3.5.2. Bedload transport rates

The height of dunes ranges from 0.14 to 0.26 m and their migration velocities from $24 \cdot 10^{-5} \text{ m s}^{-1}$ to $80 \cdot 10^{-5} \text{ m s}^{-1}$ (Table 1). At S6, celerity is at its lowest ($24 \cdot 10^{-5} \text{ m s}^{-1}$), as are the associated transport rates ($0.04\text{--}0.06 \text{ kg s}^{-1} \text{ m}^{-1}$). Similarly, the highest dune velocities

($\geq 65 \cdot 10^{-5} \text{ m s}^{-1}$) are associated with the highest transport rates ($0.13\text{--}0.23 \text{ kg s}^{-1} \text{ m}^{-1}$). For the intermediate values ($38 \cdot 10^{-5}\text{--}50 \cdot 10^{-5} \text{ m s}^{-1}$), the bedload transport rates range from 0.05 to $0.14 \text{ kg s}^{-1} \text{ m}^{-1}$, but show no direct relationship with the increase in dune celerity. The lowest transport rates were observed for discharges close to the peak of flood 1 ($527 \text{ m}^3 \text{ s}^{-1}$) and flood 3 ($797 \text{ m}^3 \text{ s}^{-1}$) and during the falling stage of the single peak of flood 2 (S6) at a discharge of $567 \text{ m}^3 \text{ s}^{-1}$. For similar discharge and steepness values for surveys S4, S5, and S11, transport rates are similar for S4 and S5 but are lower for S11.

4. Discussion

4.1. Schematic model of the nonmigrating bar and superimposed dune dynamics during floods

The identification of a dominant control parameter among stage variations, morphological context, or sediment supply remains a difficulty in understanding the dynamics of bars (Hooke and Yorke, 2011; Reesink et al., 2014). The data resolution of our study allows us to detail

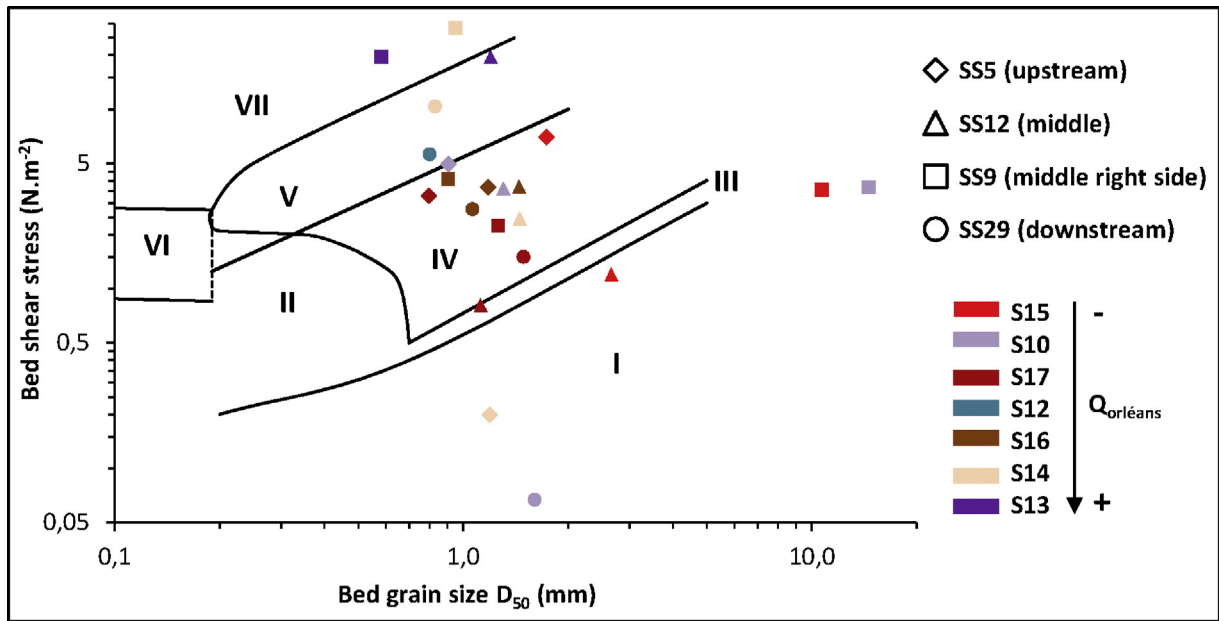


Fig. 11. D_{50} sediment bed grain size in relation to the bed shear stress plotted in the Southard and Boguchwal (1990) bedform stability diagram. Labels for region: I, no movement on plane bed; II, ripples; III, lower plane bed; IV, dunes; V, overlap region of dunes, upper plane bed, and antidunes; VI, overlap region of ripples, upper plane bed, and antidunes; VII, overlap region of upper plane bed and antidunes.

the processes occurring during a single high-magnitude flood event by proposing a conceptual model of the dynamics of a nonmigrating mid-channel bar principally forced by a static perturbation (here a riffle), which can be somehow transposed on other fluvial systems. We also discuss the effect of flood succession (of various duration and intensities) on bar dynamics and superimposed dunes.

For the sake of simplicity, two specific areas can be distinguished in terms of sediment dynamics on the nonmigrating bar studied in this paper. Namely, the upstream part of the bar appears as a relatively stable area where the presence of the riffle and armor layers stabilize the bar head. This part differs from the downstream part, margins, and bar front that are highly mobile and are characterized by relatively well-sorted sandy sediments. This can be explained by the high value of the Shields critical threshold for sediment motion parameter (as already shown on other bars of the Loire by Claude et al., 2012, and Rodrigues et al., 2015). The sedimentary processes on these two areas of the bar depend on hydrological variations (as shown by Friedman et al., 1996, and Kiss and Sipos, 2007, for other fluvial systems) and associated sediment supply (phasing, quantity, and grain size).

During a single peak of flood with magnitude higher than the flood with two years of return period, deposition processes occur at the end of the rising limb and at the beginning of the falling limb when sediments are delivered from the main channel. During a single peak flood with lower magnitude, deposition processes occur after the flood peak, during the beginning of the falling stage when sediments are supplied from the main channel. During the falling water stage, the top of the bar and the right-bank area of its front undergo erosion, while the bar spreads laterally toward the left bank (southwest) caused by the combined effects of the riffle and the slope gradient of the secondary channel. Thus, the morphological evolution and the associated sedimentary record are strongly correlated with discharge variations (as shown by Jones, 1977; Friedman et al., 1996; Best et al., 2003; Kiss and Sipos, 2007, in other contexts). Although the bar considered here is induced by the presence of a riffle, the morphological evolution of the mid-channel bar during a flood event is in line with the model proposed by Bridge (1993, 2003) with a trend for erosion of the bar margins and deposition on the top during the rising water stage and erosion of the top and lateral deposition during the falling stage. Although this general model should be slightly modified on our site

since the upstream part of the bar is fixed to the riffle, it is also in accordance with the findings of Ashworth et al. (2000) and Kiss and Sipos (2007) concerning the phasing of erosional and deposition processes occurring during a flood event as well as the role played by dunes during bar accretion (Ashworth et al., 2000; Best et al., 2003). The morphological response of the nonmigrating bar to high-magnitude floods can be described using the following five step conceptual models (Fig. 16):

- Stage 1: erosive phase, until the medium rising stage of previously deposited sediments; development of dunes from sediments previously stored on the bar; no supply from main channel.
- Stage 2: swelling phase, associated with sediment deposition on the back of the bar from lateral supply from the main channel leading to a longitudinally convex morphology near the flood peak (the bar-top continues to grow at the early stage of the flood decline).
- Stage 3: building phase, during high flow associated with sediment supply from the main channel (lateral and upstream). Elongation and lateral spreading at the end of rising and at the beginning of falling water stages (Fig. 5C). This phase led to the elongation and lateral spreading of the bar, absent for flood with lower discharge. Thus, deleting this stage allows us the use of the conceptual model for low-magnitude flood discharge.
- Stage 4: waning stage, with asymmetrical spreading and flattening of the bar caused by sediment reworking during the falling limb of the flood (S5–S6, S10–S11, and S16–S17); no resupply from the main channel.
- Stage 5: margin-reworking, erosion of the bar front and of the margins when the bar is disconnected. The spatial extension of the bar thus reduces considerably compared to higher discharge conditions.

The influence of the swelling of the bar on flow resistance was not tested in this study but should be done in the future. This process can modify the boundary layer and the development of dunes on migrating bars (Carling et al., 2000; Claude et al., 2014) and on point bars (Dietrich and Smith, 1984).

The succession of peak discharges during multiplex floods or time intervals between floods also influence the nonmigrating bar morphology. For instance, the bar's back morphology inherited at the end of a falling

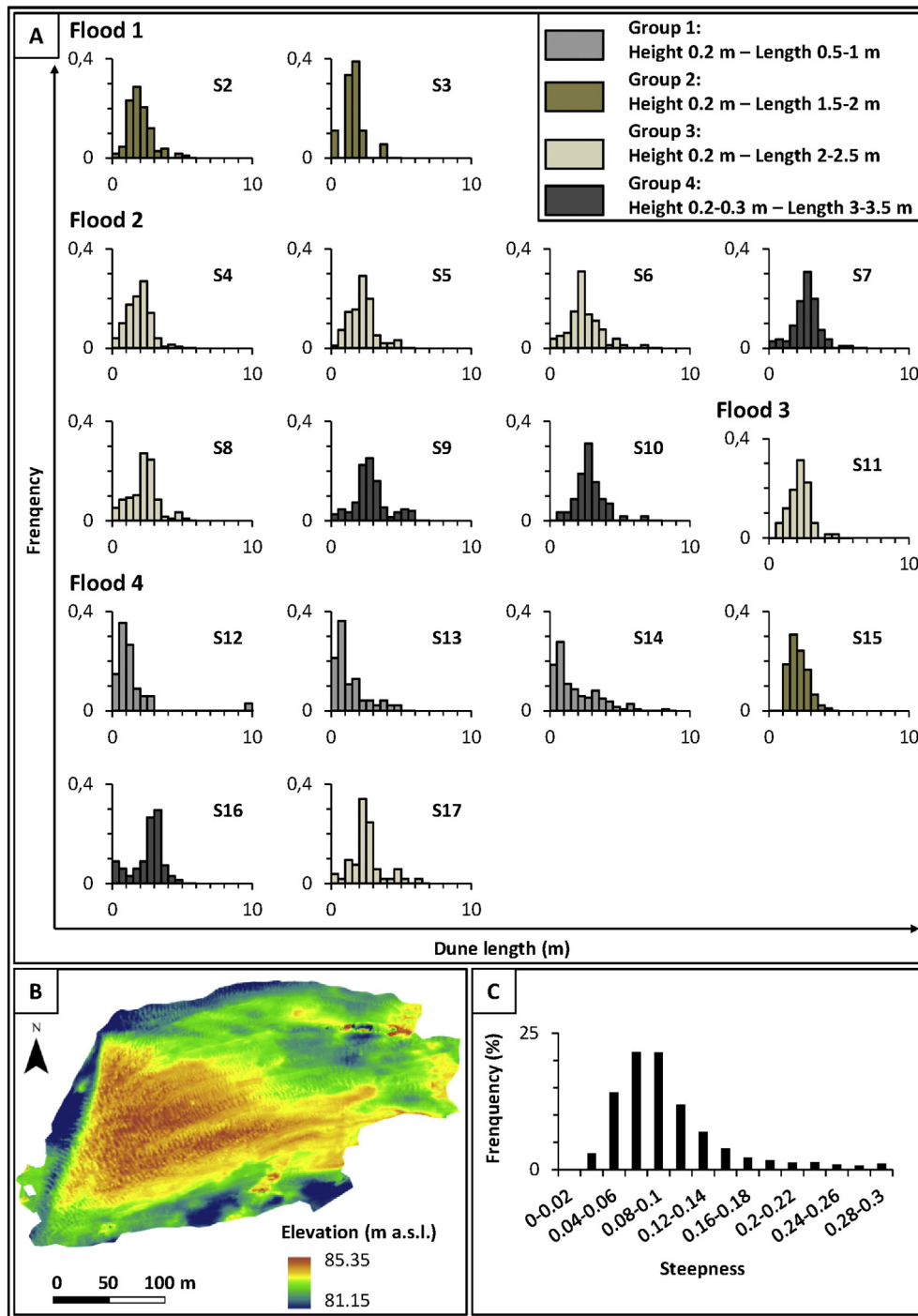


Fig. 12. Frequency of dunes length for each survey (A), the number of dune is available in [Table 1](#). Digital elevation model during the high-magnitude flood (S14) with discharge of $1810 \text{ m}^3 \text{ s}^{-1}$ (B). Frequency of steepness for all dunes measured with the whole surveys.

limb is preserved at the beginning of the subsequent one if the decline between the two peaks does not drive to the emersion of the bar. Then, the bar's back evolves from this inherited morphology. As a consequence, the succession of flood peaks allows the swelling of the bar's back avoiding the occurrence of stage 5 (mainly associated with the emersion of the bar). Thus, two key parameters affect the morphological evolution of the nonmigrating, mid-channel bar during successive floods: (i) the duration of falling limbs determining the inherited morphology (convex or flat), and (ii) the emersion of the bar leading to the bar-top flattening and front bar retreat by erosion.

During flood events, the balance between deposited and eroded volumes on CS6 to CS16 highlights a state of either a negative or positive

sediment budget compared to the initial state. [Fig. 17](#) indirectly represents the gradient of sediment transport rate over the bar. Although the relationship between sediment transport rates and sediment budget is not linear, the rapid increase in sediment budget noted for floods 2 and 4 highlights a significant sediment deposition coming from the main channel. After long or high amplitude falling limbs the bar tends to show a negative budget, which is not always compensated for by sediment supplied in the subsequent flood. Overall, for the study period, the bar sediment budget is often negative compared to the initial post-engineering work state ([Fig. 17](#)). These results lead us to the conclusion that during low-intensity floods, sediment supply is lower than during the high-intensity events as shown by [Rodrigues et al.](#)

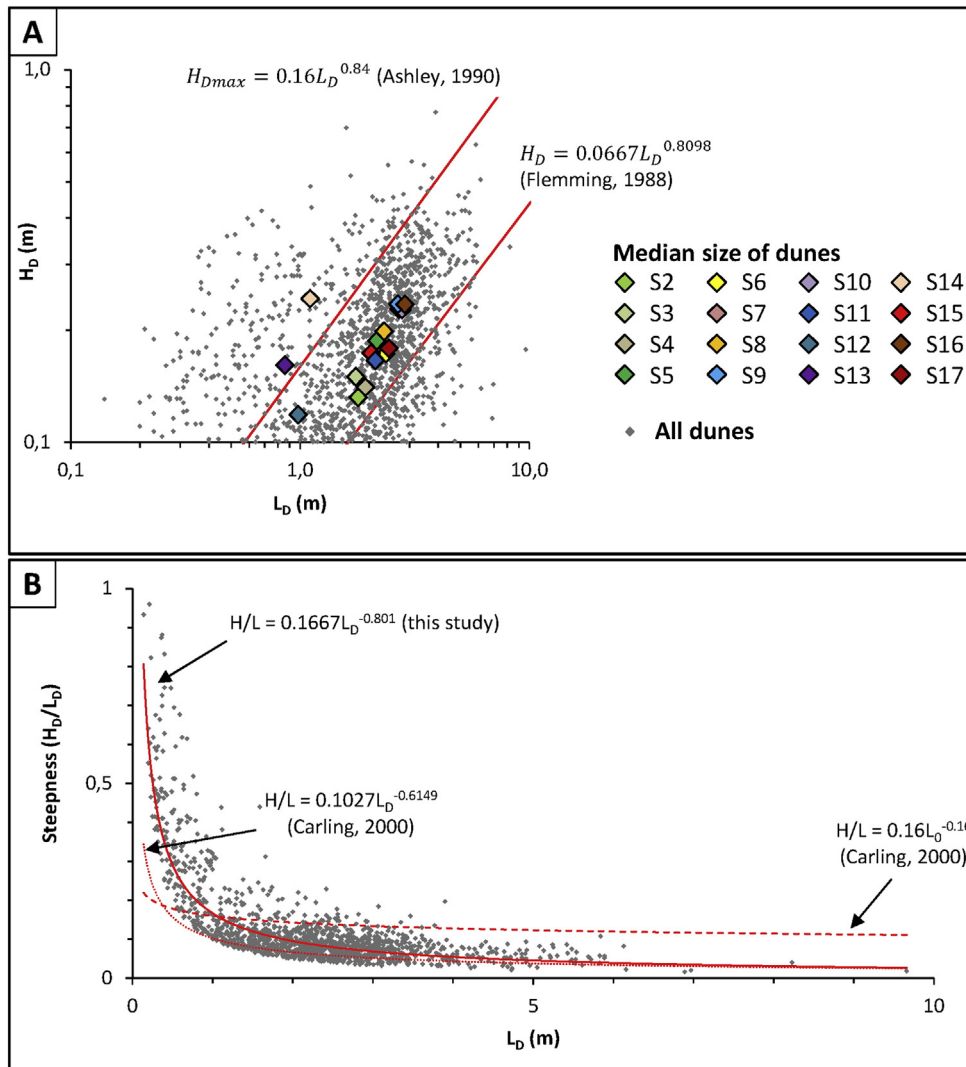


Fig. 13. Total and median dune wavelengths and heights compared to the theoretical equations of Flemming (1988) and Ashley (1990)(A). Steepness evolution in regard to dune lengths compared to Carling et al. (2000) results on the River Rhine (B). (n = 1423).

(2006) on a nonmigrating bar located in an inlet of a side channel of the Loire.

As mentioned above, the flood stage and the phasing of sediment supply have a major influence on the morphology of the nonmigrating bar and on dune development. This latter is influenced by several potential limiting factors such as the water depth, the balance between sediment grain size, bed shear stress, and sediment availability (depending on sediment supply from the main channel, armor layer formation, and the presence of a previously deposited sediment store).

The initial morphology of the bar resulting from the fluvial management works (vegetation removal, topographical lowering, and sediment mixing) influenced the dune development. During the first flood after management works, dunes developed from the sediment store represented by the low-elevation, flattened bar surface with mixed sediments in a regressive way (upstream-oriented process).

Firstly, dunes appeared on the front of the bar (which was subject to spreading) and also during the first peak of the second flood, whereas no significant sediment supply from the main channel was recorded on the bathymetrical data. This suggests that, initially, dunes developed from the sandy sediments of the downstream part of the bar in a context of sediment deficit (and independently of the low sediment supply coming from the main channel). Kleinhans et al. (2002) suggested that the sediment deficit for bedforms to develop can depend on the

grain sizes constituting the river bed, which are sometimes too large to be mobilized; this can explain why dunes do not develop in the middle part of the bar. However, the absence of dunes in the upstream part could be induced by a thin active layer owing to the nonalluvial bed marked by the natural riffle. This part remains without dunes throughout the study. For low discharge conditions, our results suggest that the predominant factor of dunes development is the sediment availability and grain size. The development of relatively small dunes regular in shape and size suggests a limited sediment supply or a thin active layer (Dalrymple and Rhodes, 1995; Tuijnder et al., 2009). The armor layer development also suggests a context of sediment deficit. According to Carling et al. (2000), even in a context of sediment deficit, dune height can continue to grow to the detriment of their length, and this was observed just before the peak of flood 4 (S12). Furthermore, Kleinhans et al. (2002) and Tuijnder et al. (2009) showed that under limited sediment supply conditions dune size was independent of water depth and flow velocity.

Secondly, the massive sediment supply delivered by the main channel at the end of the rising limb or at the onset of the falling limb of high-magnitude floods (i.e., flood 4) influenced the dune dynamics. These hydrological events have provided enough sediment for dune development that was only limited by the balance between bed shear stress and critical shear stress. The hysteretic process linked to variation

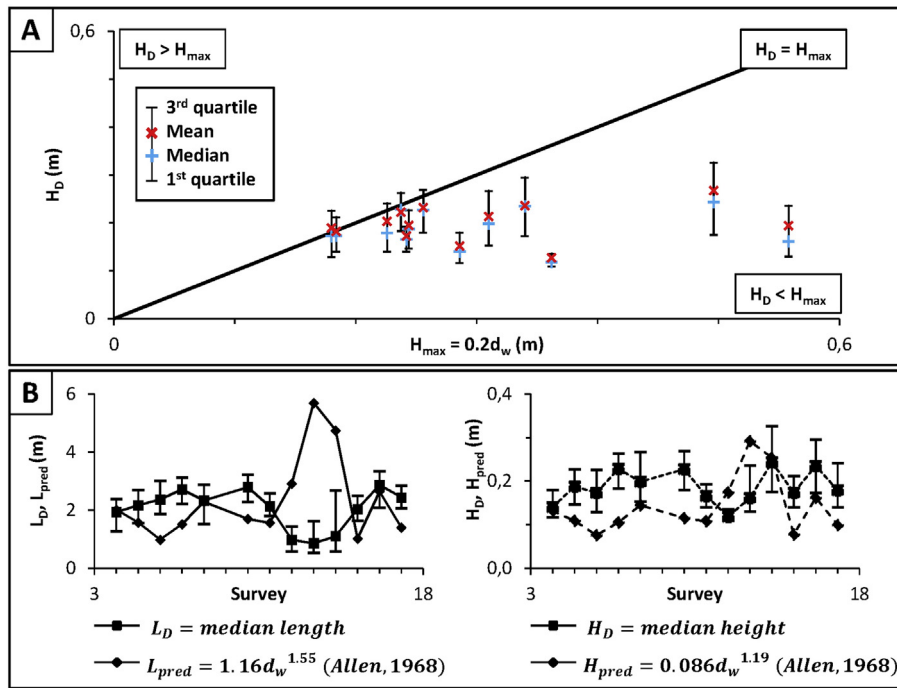


Fig. 14. (A) Dune height for each survey according to the maximum development height of dunes in rivers estimated at 20% of water depth (Kleinhans et al., 2002). (B) Comparison between median dune lengths (L_D) and median dune heights (H_D) per measurement survey with predicted values (L_{pred} and H_{pred}) using Allen (1968)'s equilibrium model. The error bars represent the quartiles calculated around the median.

in discharge, and showing a faster response in dune height than in dune length, complicates the analysis of the abovementioned limiting factors on dune growth. The rapid increase in dune height just after the peak of F4 and its subsequent decrease is in phase with the sediment supply delivered by the main channel. Apparently, dunes adapted to the massive sediment supply firstly by modifying their height and afterward by increasing their length at the end of the flood (while their height decreased probably because of the decrease in sediment supply). Under nonlimiting sediment availability conditions, the difficulty that the dunes had to grow in our system could be linked to the wide grain-size range and the often bimodal character of the sediment (Kleinhans et al., 2002). Our results show that, on a mid-channel, nonmigrating bar developed in a sandy-gravel bed of a lowland river, superimposed dune growth is mainly influenced by sediment supply, grain size, flow strength, and in a lesser way, water depth (as shown by Bartholdy et al., 2005, in a tidal environment).

The identification of dunes along longitudinal track LT18 allowed us to apply the dune tracking method to calculate bedload transport rates. They are comparable to those calculated in the main channel of the Loire River by Claude et al. (2012). According to the migration rates measured and to Kuhnle et al. (2006), superimposition and amalgamation of dunes was not observable in our system.

4.2. Influence of hydrology on forcing parameters inducing a nonmigrating bar

The results presented herein highlight a hydrological control of the morphological forcing parameters that govern the presence and the dynamics of the nonmigrating bar. These forcing parameters are (i) the presence of a stationary obstacle (riffle), (ii) an expansion area, and (iii) a low-curvature degree in the channel planform. Hereafter, points 2 and 3 will be referred as planform forcing. On the study site, as for other rivers, the effects of these parameters interact one to each other. In other words, the presence of the riffle is responsible for the expansion area and the building of vegetated islands in this part of the Loire. In that sense, the obstacle (here the riffle) could be interpreted as a first-degree forcing parameter, whereas expansion area and the vegetated islands are consequences that also influence the bar dynamics.

During low and medium flows, the effect on the morphological setting (riffles, vegetated islands, etc.) is stronger than during high-flow periods. For low-flow conditions, the natural riffles, the expansion area, and the vegetated islands influence elevation and slope of the water surface as well as flow direction and velocity. The two riffles present in the main channel (Fig. 1) reduce the water surface slope and then promote a lateral gradient toward the side channel (Fig. 3)

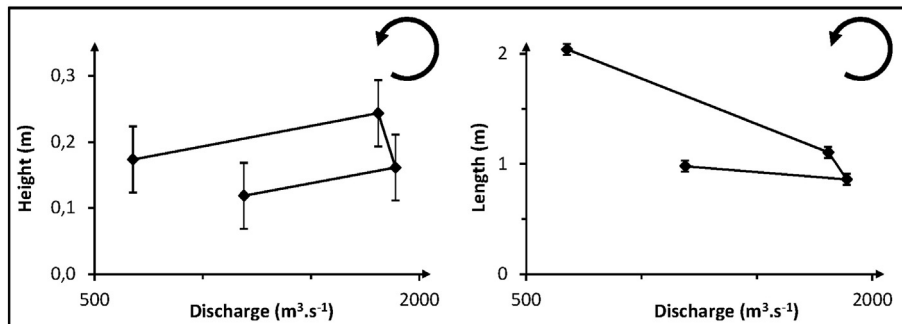


Fig. 15. Evolution of dune heights and lengths in regard to the modification of discharge and water depth during the high-magnitude flood surveyed.

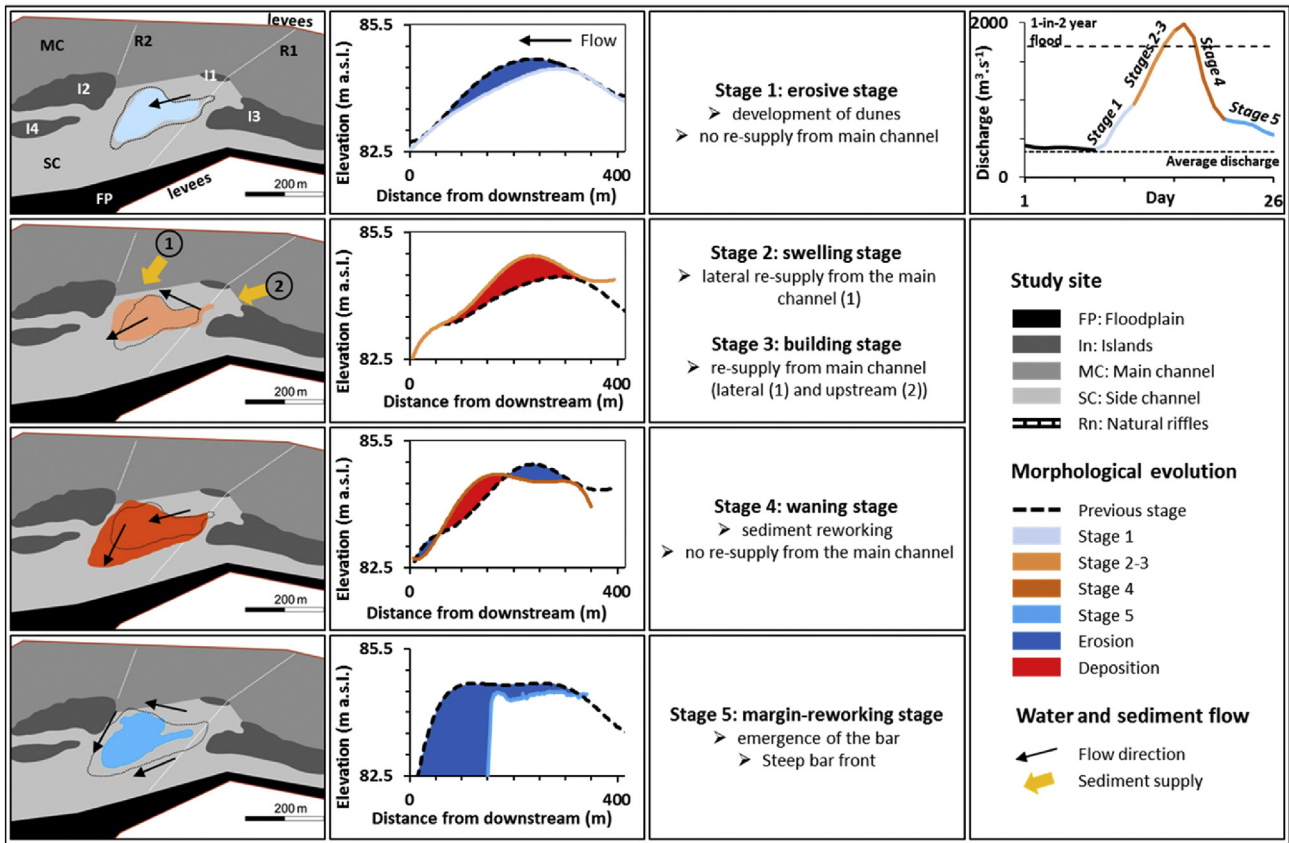


Fig. 16. Conceptual model of the morphological evolution of the nonmigrating bar (planform and bathymetry) during a flood event. On maps, black dashed lines correspond to the previous stage, whereas colored bars refer to the evolution stage. Longitudinal tracks correspond to LT18 and the color code refers to the maps. Stages 2 and 3 are grouped because they refer to sediment supply (different according to the flood magnitude).

responsible for the spreading of the bar toward the left bank during low flows.

During high-flow periods, the effects of the riffle on flow decreases. Contrarily, the role of planform forcing parameters (expansion area and low degree of curvature) becomes higher (Fig. 18). For these water levels, flow is deflected toward the right bank. The divergence of flow for discharges higher than the 1-in-2 year flood induces a sediment deposition and a spreading of the bar in this direction. This sediment deposition can afterward be colonized by vegetation and evolve as vegetated

islands (i.e., I1 and I2, Fig. 1) which also interacts with the nonmigrating bar by splitting the flow and sediment supply (I1, Fig. 1) or by inducing, during the falling limb of the flood, the formation of a small channel responsible for the lateral scouring of the margins of the bar after its spreading during floods.

Nonmigrating bars can lead to the morphological evolution of river beds (Parker, 1976; Hooke and Yorke, 2011; Van Dijk, 2013). For instance, nonmigrating bars such as point bars explain the overdeepening process occurring along the outer bank of rivers, which is responsible for

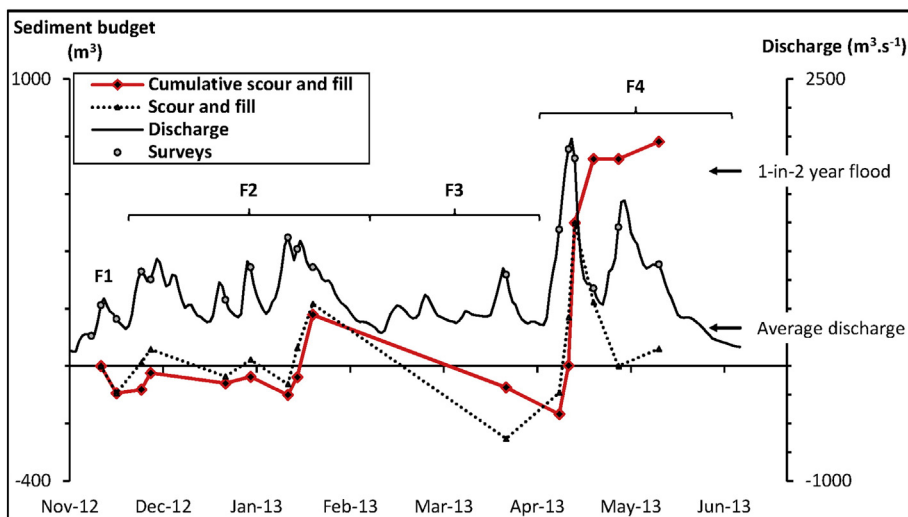


Fig. 17. Evolution over time according to discharge rates of deposited and eroded volumes and of cumulative volumes on CS6–CS16.

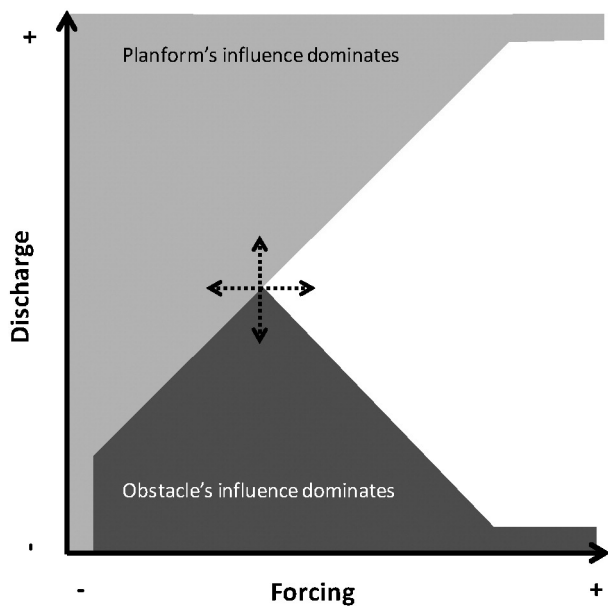


Fig. 18. Theoretical view (based on this study) of the hydrological control of the morphological forcing parameters (obstacle [riffle] vs. planform [expansion and low-amplitude curvature]) involved in the dynamics of nonmigrating bars. Arrows indicate that the relative influence of the two morphological forcing parameters can shift according to the specificity of the site considered.

the lateral migration of meander bends (Struiksmá et al., 1985; Parker and Johannesson, 1989) modulated by hydrology, bank geotechnical characteristics, and riparian vegetation (Nanson and Beach, 1977; Hooke and Yorke, 2011).

Results presented in this paper suggest that nonmigrating bars forced by a steady local perturbation (i.e., a riffle) can be responsible for some local morphological evolution (specifically on the erosion of islands located close to the bar) but do not drive to a significant morphological evolution of the river reach because of their fixed position in the channel. Classically, if the banks of the reach were easily erodible (which is not the case here because of the presence of levees), they would retreat during the low migration of the bar inducing a general morphological adjustment of the channel (Coleman, 1969; Klaassen and Masselink, 1992; Thorne et al., 1993; Ashworth et al., 2000). This process was observed on several fluvial systems of various sizes and can be associated with the divergence of flows induced by the expansion area, which can be involved in the development of secondary helical flows present in the surrounding channels (Whiting and Dietrich, 1991; Bridge and Gabel, 1992; Bridge, 1993; Richardson et al., 1996; Richardson and Thorne, 1998). Contrary to a point bar or even to some migrating bars present in meandering channels (Hooke and Yorke, 2011), an obstacle-induced bar will not translate laterally as its formation is linked to the presence of a static perturbation. However, the morphological influence of this bar type on the river reach can increase with time as it constitutes a potential site of woody vegetation recruitment and island edification. If the bar evolves as an established island, its influence on flow, sediment transport, and local morphological evolution will increase with time (McKenney et al., 1995; Gurnell et al., 2001). In other words, the life-cycle (see Hooke and Yorke, 2011) of two nonmigrating bars (induced by a steady perturbation or by planform) will be different according to their cause of formation.

5. Conclusions

This study was conducted on the Loire River (France) on a nonmigrating, mid-channel bar forced by a riffle and planform changes (local channel widening and low sinuosity). Based on a large data set acquired after management works that ensured an initial flat bed and

a homogenized grain-size distribution, we propose a conceptual model of nonmigrating bar dynamics during floods, detailing the interactions with superimposed dunes. The model proves that, in a relatively large lowland sandy-gravel bed river, the dynamics of a nonmigrating, mid-channel bar forced by a riffle can be resumed to a rather stable area that constitutes some type of nucleus around which spreading (bar margins), elongation (bar front), and swelling (bar back) occur and during flood events. During the falling limb of floods, sediments deposited on the top of the bar and on the bar front are reworked; a lateral spreading toward a side channel was also shown. When water leaves the bar, significant lateral erosion of the bar margin occurs. Dunes developed instantaneously from the flat surface created during management works during the first flood by an upstream-oriented process. Dune development strongly depends on sediment (phasing, quantity, and grain size) supplied by the surrounding channels during high-magnitude floods and by sediment availability (governed by armor layers and non alluvial parts) during low-flow stages. The size and shape of dunes were rather stable even if adaptations were noted according to a weak anticlockwise hysteresis. This study shows that superimposed dune growth is mainly influenced by sediment supply, grain size, flow strength, and in a lesser way water depth.

Morphological forcing parameters (steady perturbation [riffle] vs. planform [widening, channel curvature]) govern the presence, the dynamics of the nonmigrating bar and its long-term evolution. The role of these parameters on bar dynamics is cumulative but to a certain extent stage dependant. For low discharges, the influence of the riffle dominates (specifically on local flows). During high-flow stages it influences sediment availability, but flow direction and strength are rather influenced by planform parameters.

This study is a first step to understand interactions between a nonmigrating, mid-channel bar forced by a steady perturbation (riffle) and superimposed dunes during unsteady flows. As a sedimentological perspective, the analysis of the influence of the location of dunes on the bar (front/back) on their development and morphological evolution should be done.

Acknowledgments

This study is part of the Ph.D. thesis of the first author and is funded by the Master Plan Loire Grandeur Nature – FEDER (Presage no. 34971), Agence de l'Eau Loire-Bretagne (no. 100392601), Etablissement Public Loire (11-DR-RD-015), and Région Centre. Michel Chantereau, Damien Hemeray (Réserve Naturelle Saint-Mesmin), and Thomas Carrière (DDT 45) are acknowledged for their valuable help. Y. Guerez and T. Handfus (CETU ELMIS – University of Tours) are thanked for their help during flood surveys. Other field investigations and grain size analysis were carried out with the help of J.-P. Bakyono, I. Pene, and M. Rincel (University F. Rabelais, Tours). O. Ursache (University F. Rabelais, Tours) is acknowledged for his help during the analysis of hydraulic data. The authors are particularly keen to thank A.J. Reesink for his proofreading work which improved the manuscript structure and so the scientific message transmission. The authors are grateful to the reviewers for their useful comments that improved the paper. The authors wish to thank Sue Edrich for the English translation of the manuscript.

The revisions were made when the first author was a visiting fellow at the University of Western Ontario (Canada) welcomed by Pr. Peter Ashmore.

References

- Allen, J.R.L., 1968. *Current Ripples – Their Relation to Patterns of Water and Sediment Motion*. North-Holland Publishing Company, Amsterdam (433 pp.).
- Ashley, G.M., 1990. Classification of large-scale subaqueous bedforms; a new look at an old problem. *J. Sediment. Res.* 60, 160–172. <http://dx.doi.org/10.2110/jsr.60.160>.
- Ashmore, P.E., 1982. Laboratory modelling of gravel braided stream morphology. *Earth Surf. Process. Landf.* 7, 201–225. <http://dx.doi.org/10.1002/esp.3290070301>.
- Ashmore, P.E., 1991. How do gravel-bed rivers braid. *Can. J. Earth Sci.* 28, 326–341. <http://dx.doi.org/10.1139/e91-030>.

- Ashworth, P.J., 1996. Mid-channel bar growth and its relationship to local flow strength and direction. *Earth Surf. Process. Landf.* 21, 103–123. [http://dx.doi.org/10.1002/\(SICI\)1096-9837\(199602\)21:2<103::AID-ESP569>3.0.CO;2-O](http://dx.doi.org/10.1002/(SICI)1096-9837(199602)21:2<103::AID-ESP569>3.0.CO;2-O).
- Ashworth, P.J., Ferguson, R.L., Ashmore, P.E., Paola, C., Powell, D.M., Prestegaaers, K.L., 1992. Measurements in a Braided River chute and lobe: 2. Sorting of bed load during entrainment, transport, and deposition. *Water Resour. Res.* 28, 1887–1896. <http://dx.doi.org/10.1029/92WR00702>.
- Ashworth, P.J., Best, J.L., Roden, J.E., Bristow, C.S., Klaassen, G.J., 2000. Morphological evolution and dynamics of a large, sand braid-bar, Jamuna River, Bangladesh. *Sedimentology* 47, 533–555. <http://dx.doi.org/10.1046/j.1365-3091.2000.00305.x>.
- Bartholdy, J., Flemming, B.W., Bartholomä, A., Ernstsens, V.B., 2005. Flow and grain size control of depth-independent simple subaqueous dunes. *J. Geophys. Res.* 110, F04S16 (12 pp.).
- Best, J.L., Ashworth, P.J., Bristow, C.S., Roden, J.E., 2003. Three-dimensional sedimentary architecture of a large, mid-channel sand braid bar, Jamuna River, Bangladesh. *J. Sediment. Res.* 73 (4), 516–530. <http://dx.doi.org/10.1306/010603730516>.
- Bittner, L.D., 1994. *River Bed Response to Channel Width Variations: Theory and Experiments*. University of Illinois, Urbana-Champaign.
- Blondeaux, P., Seminara, G., 1985. A unified bar-bend theory of river meanders. *J. Fluid Mech.* 157, 449–470. <http://dx.doi.org/10.1017/S0022112085002440>.
- Blott, S.J., Pye, K., 2001. GRADISTAT: a grain size distribution and statistics package for the analysis of unconsolidated sediments. *Earth Surf. Process. Landf.* 26, 1237–1248. <http://dx.doi.org/10.1002/esp.261>.
- Bridge, J.S., 1993. The interaction between channel geometry, water flow, sediment transport and deposition in braided rivers. In: Best, J.L., Bristow, C.S. (Eds.), *Braided Rivers*. Geological Society Special Publication, London, pp. 13–71.
- Bridge, J.S., 2003. *Rivers and Floodplains: Forms, Processes, and Sedimentary Record*. Blackwell, Oxford (491 pp.).
- Bridge, J.S., Best, J.L., 1988. Flow, sediment transport and bedform dynamics over the transition from dunes to upper stage plane beds. *Sedimentology* 35, 753–764.
- Bridge, J.S., Gabel, S.L., 1992. Flow and sediment dynamics in a low sinuosity, braided river: Calamus River, Nebraska Sandhills. *Sedimentology* 39, 125–142. <http://dx.doi.org/10.1111/j.1365-3091.1992.tb01026.x>.
- Bristow, C.S., 1987. Brahmaputra River: channel migration and deposition. In: Ethridge, F.G., Flores, R.M., Harvey, M.D. (Eds.), *Recent Developments in Fluvial Sedimentology*. SEPM, Special Publications 39, pp. 63–74.
- Callander, R.A., 1969. Instability and river channels. *J. Fluid Mech.* 36, 465–480. <http://dx.doi.org/10.1017/S0022112069001765>.
- Carling, P.A., Golz, E., Orr, H.G., Radecki-Pawlik, A., 2000. The morphodynamics of fluvial sand dunes in the River Rhine, near Mainz, Germany. I. Sedimentology and morphology. *Sedimentology* 47, 227–252. <http://dx.doi.org/10.1046/j.1365-3091.2000.00290.x>.
- Claude, N., Rodrigues, S., Bustillo, V., Bréhéret, J.G., Macaire, J.J., Jugé, P., 2012. Estimating bedload transport in a large sand–gravel bed river from direct sampling, dune tracking and empirical formulas. *Geomorphology* 179, 40–57. <http://dx.doi.org/10.1016/j.geomorph.2012.07.030>.
- Claude, N., Rodrigues, S., Bustillo, V., Bréhéret, J.G., Tassi, P., Jugé, P., 2014. Interactions between flow structure and morphodynamic of bars in a channel expansion/contraction, Loire River, France. *Water Resour. Res.* 50, 2850–2873. <http://dx.doi.org/10.1002/2013WR015182>.
- Coleman, J.M., 1969. Brahmaputra River: channel processes and sedimentation. *Sediment. Geol.* 3, 129–239. [http://dx.doi.org/10.1016/0037-0738\(69\)90010-4](http://dx.doi.org/10.1016/0037-0738(69)90010-4).
- Colombini, M., Seminara, G., Tubino, M., 1987. Finite-amplitude alternate bars. *J. Fluid Mech.* 181, 213–232. <http://dx.doi.org/10.1017/S0022112087002064>.
- Crosato, A., Mosselman, E., 2009. Simple physics-based predictor for the number of river bars and the transition between meandering and braiding. *Water Resour. Res.* 45, W03424. <http://dx.doi.org/10.1029/2008WR007242>.
- Crosato, A., Desta, F.B., Cornelisse, J., Schuurman, F., Uijtewaal, W.S.J., 2012. Experimental and numerical findings on the long-term evolution of migrating alternate bars in alluvial channels. *Water Resour. Res.* 48, W06524. <http://dx.doi.org/10.1029/2011WR011320>.
- Dachary, M., 1996. Les grandes crues historiques de la Loire. La Houille Blanche 6–7, 47–53. <http://dx.doi.org/10.1051/lhb/1996067>.
- Dalrymple, R.W., Rhodes, R.N., 1995. Estuarine dunes and bars. In: Perillo, G.M.E. (Ed.), *Geomorphology and Sedimentology of Estuaries*. Developments in Sedimentology 53. Elsevier, ISBN: 9789400701236, pp. 359–422 (9400701233).
- Dietrich, W.E., Smith, J.D., 1984. Bed load transport in a river meander. *Water Resour. Res.* 20, 1355–1380.
- Dinehart, R.L., Burau, J.R., 2005a. Averaged indicators of secondary flow in repeated acoustic Doppler current profiler crossings of bends. *Water Resour. Res.* 41, W09405. <http://dx.doi.org/10.1029/2005WR004050>.
- Dinehart, R.L., Burau, J.R., 2005b. Repeated surveys by acoustic Doppler current profiler for flow and sediment dynamics in a tidal river. *J. Hydrol.* 314, 1–21. <http://dx.doi.org/10.1016/j.jhydrol.2005.03.D.019>.
- Eekhout, J.P.C., Hoiink, A.J.F., Mosselman, E., 2013. Field experiment on alternate bar development in a straight sand-bed stream. *Water Resour. Res.* 49, 8357–8369. <http://dx.doi.org/10.1002/2013WR014259>.
- Federici, B., Paola, C., 2003. Dynamics of channel bifurcations in noncohesive sediments. *Water Resour. Res.* 39, 1162. <http://dx.doi.org/10.1029/2002WR001434>.
- Flemming, B.W., 1988. Zur klassifikation subaquatischer, strömungstransversaler transportkörper. *Bochumer geologische und geotechnische arbeiten* 29, 44–47.
- Flemming, B.W., 2000. The role of grain size, water depth and flow velocity as scaling factors controlling the size of subaqueous dunes. *Marine Sandwave Dynamics, Proceedings of an International Workshop, Lille (France)*, pp. 55–60.
- Friedman, J.M., Osterkamp, W.R., Lewis, W.M., 1996. The role of vegetation and bed-level fluctuations in the process of channel narrowing. *Geomorphology* 14, 341–351. [http://dx.doi.org/10.1016/0169-555X\(95\)00047-9](http://dx.doi.org/10.1016/0169-555X(95)00047-9).
- Gaeuman, D., Jacobson, R.B., 2007. Field assessment of alternative bed-load transport estimators. *J. Hydraul. Eng.* 133, 1319. [http://dx.doi.org/10.1061/\(ASCE\)0733-9429\(2007\)133:12\(1319\)](http://dx.doi.org/10.1061/(ASCE)0733-9429(2007)133:12(1319)).
- Gurnell, A.M., Petts, G.E., Hannah, D.M., Smith, B.P.G., Edwards, P.J., Kollmann, J., Ward, J.V., Tockner, K., 2001. *Riparian vegetation and island formation along the gravel-bed Fiume Tagliamento, Italy*. *Earth Surf. Process. Landf.* 26, 31–62.
- Hoekstra, P., Bell, P., Van Santen, P., Roode, N., Levoy, F., Whitehouse, R., 2004. Bedform migration and bedload transport on an intertidal shoal. *Cont. Shelf Res.* 24, 1249–1269. <http://dx.doi.org/10.1016/j.csr.2004.03.006>.
- Hooke, J., Yorke, L., 2011. Channel bar dynamics on multi-decadal timescales in an active meandering river. *Earth Surf. Process. Landf.* 36, 1910–1928.
- Jackson, R.G., 1975. Hierarchical attributes and a unifying model of bed forms composed of cohesionless material and produced by shearing flow. *Bull. Geol. Soc. Am.* 86, 1523–1533. [http://dx.doi.org/10.1130/0016-7606\(1975\)86<1523:HAAUM>2.0.CO;2](http://dx.doi.org/10.1130/0016-7606(1975)86<1523:HAAUM>2.0.CO;2).
- Jones, C.M., 1977. Effects of varying discharge regimes on bed-form sedimentary structures in modern rivers. *Geology* 5, 567–570.
- Kiss, T., Sipos, G., 2007. Braid-scale channel geometry changes in a sand-bedded river: significance of low stages. *Geomorphology* 84, 209–221. <http://dx.doi.org/10.1016/j.geomorph.2006.01.041>.
- Klaassen, G.J., Masselink, G., 1992. Planform changes of a braided river with fine sand as bed and bank material. *Proceedings 5th International Symposium on River Sedimentation, Karlsruhe, Germany*, pp. 459–471.
- Kleinhans, M.G., Van Den Berg, J.H., 2011. River channel and bar patterns explained and predicted by an empirical and a physics-based method. *Earth Surf. Process. Landf.* 36, 721–738. <http://dx.doi.org/10.1002/esp.2090>.
- Kleinhans, M.G., Wilbers, A.W.E., De Swaaf, A., Van Den Berg, J.H., 2002. Sediment supply-limited bedforms in sand–gravel bed rivers. *J. Sediment. Res.* 72, 629–640. <http://dx.doi.org/10.1306/030702720629>.
- Kostaschuk, R., Best, J., 2005. Response of sand dunes to variations in tidal flow: Fraser Estuary, Canada. *J. Geophys. Res.* 110, F04S04. <http://dx.doi.org/10.1029/2004JF000176>.
- Kostaschuk, R.A., Church, M.A., Luternauer, J.L., 1989. Bedforms, bed material, and bedload transport in a salt-wedge estuary: Fraser River, British Columbia. *Can. J. Earth Sci.* 26, 1440–1452. <http://dx.doi.org/10.1139/e89-122>.
- Kuhnle, R.A., Horton, J.K., Bennett, S.J., Best, J.L., 2006. Bed forms in bimodal sand–gravel sediments: laboratory and field analysis. *Sedimentology* 53, 631–654. <http://dx.doi.org/10.1111/j.1365-3091.2005.00765.x>.
- Lanzoni, S., 2000a. Experiments on bar formation in a straight flume: 1. Uniform sediment. *Water Resour. Res.* 36, 3337–3349. <http://dx.doi.org/10.1029/2000WR900160>.
- Lanzoni, S., 2000b. Experiments on bar formation in a straight flume: 2. Graded sediment. *Water Resour. Res.* 36, 3351–3363. <http://dx.doi.org/10.1029/2000WR900161>.
- Latapie, A., 2011. *Modélisation de l'évolution morphologique d'un lit alluvial: exemple de la Loire Moyenne (Thèse)*, Université François Rabelais de Tours, France (279 pp.).
- Latapie, A., Camenen, B., Rodrigues, S., Paquier, A., Bouchard, J.P., Moatar, F., 2014. Assessing channel response of a long river influenced by human disturbance. *Catena* 121, 1–12. <http://dx.doi.org/10.1016/j.catena.2014.04.017>.
- Leopold, L.B., Wolman, M.G., 1957. *River channel patterns: braided, meandering, and straight*. United States Geophysical Survey, Professional Paper 262-B.
- Macaire, J.J., Gay-Ovejero, I., Bacchi, M., Cocirta, C., Patryl, L., Rodrigues, S., 2013. Petrography of alluvial sands as a past and present environmental indicator: case of the Loire River (France). *Int. J. Sediment Res.* 28, 285–303. [http://dx.doi.org/10.1016/S1001-6279\(13\)60040-2](http://dx.doi.org/10.1016/S1001-6279(13)60040-2).
- McKenney, R., Jacobson, R.B., Wertheimer, R.C., 1995. Woody vegetation and channel morphogenesis in low gradient, gravelled streams in the Ozark Plateaus, Missouri and Arkansas. *Geomorphology* 13, 175–198.
- McLelland, S.J., Ashworth, P.J., Best, J.L., Roden, J., Klaassen, G.J., 1999. *Flow Structure and Transport of Sand-Grade Suspended Sediment around an Evolving Braid Bar, Jamuna River, Bangladesh*. In: Smith, N.D., Rogers, J. (Eds.), *Fluvial Sedimentology VI: International Association of Sedimentologists Special Publication 28*. Blackwell Publishing Ltd., pp. 43–57.
- Miori, S., Repetto, R., Tubino, M., 2006. A one-dimensional model of bifurcations in gravel-bed channels with erodible banks. *Water Resour. Res.* 42, W11413.
- Mosselman, E., Tubino, M., Zolezzi, G., 2006. The overdeepening theory in river morphodynamics: two decades of shifting interpretations. *Proceedings of the International Conference on Fluvial Hydraulics – River Flow 2006*, pp. 1175–1181.
- Nanson, G.C., Beach, H.F., 1977. Forest succession and sedimentation on a meandering river floodplain, northeast British Columbia, Canada. *J. Biogeogr.* 4, 229–251. <http://dx.doi.org/10.2307/3038059>.
- Naqshband, S., 2014. *Morphodynamics of River Dunes: Suspended Sediment Transport Along Mobile Dunes and Dune Development Towards Upper Stage Plane Bed (PhD thesis)*. University of Twente (149 pp.).
- Parker, G., 1976. On the cause and characteristic scales of meandering and braiding in rivers. *J. Fluid Mech.* 76, 457–480. <http://dx.doi.org/10.1017/S0022112076000748>.
- Parker, G., Johanneson, H., 1989. Observations on several recent theories of resonance and overdeepening in meandering channels. In: Ikeda, S., Parker, G. (Eds.), *River Meandering*. AGU, Water Resources Monograph 12, pp. 379–415.
- Peters, J.J., 1978. Discharge and sand transport in the braided zone of the Zaire estuary. *Neth. J. Sea Res.* 12, 273–292.
- Peters, J.J., Sterling, A., 1975. *Mateba 12: la méthode des dragages dirigés*. Laboratoire de recherches hydrauliques.
- Pinto Martins, D., Bravard, J.P., Stevaux, J.C., 2009. Dynamics of water flow and sediments in the upper Paraná River between Porto Primavera and Itaipu Dams, Brazil. *Lat. Am. J. Sedimentol. Basin Anal.* 16, 111–118.
- Reesink, A.J.H., Bridge, J.S., 2007. Influence of superimposed bedforms and flow unsteadiness on formation of cross strata in dunes and unit bars. *Sediment. Geol.* 202, 281–296. <http://dx.doi.org/10.1016/j.sedgeo.2007.02.005>.

- Reesink, A.J.H., Bridge, J.S., 2009. Influence of superimposed bedforms and flow unsteadiness on formation of cross strata in dunes and unit bars – part 2, further experiments. *Sediment. Geol.* 222, 274–300. <http://dx.doi.org/10.1016/j.sedgeo.2009.09.014>.
- Reesink, A.J.H., Bridge, J.S., 2011. Evidence of bedform superimposition and flow unsteadiness in unit-bar deposits, South Saskatchewan River, Canada. *J. Sediment. Res.* 81 (11), 814–840. <http://dx.doi.org/10.2110/jsr.2011.69>.
- Reesink, A.J.H., Ashworth, P.J., Sambrook Smith, G.H., Best, J.L., Parsons, D.R., Amsler, M.L., Hardy, R.J., Lane, S.N., Nicholas, A.P., Orfeo, O., Sandbach, S.D., Simpson, C.J., Szupiany, R.N., 2014. Scales and causes of heterogeneity in bars in a large multi-channel river: Rio Parana, Argentina. *Sedimentology* <http://dx.doi.org/10.1111/sed.12092>.
- Rennie, C.D., Church, M., 2010. Mapping spatial distributions and uncertainty of water and sediment flux in a large gravel bed river reach using an acoustic Doppler current profiler. *J. Geophys. Res.* 115, F03035. <http://dx.doi.org/10.1029/2009JF001556>.
- Repetto, R., Tubino, M., Paola, C., 2002. Planimetric instability of channels with variable width. *J. Fluid Mech.* 457, 79–109.
- Richardson, W.R., Thorne, C.R., 1998. Secondary currents around Braid Bar in Brahmaputra River, Bangladesh. *J. Hydraul. Eng.* 124, 325–327.
- Richardson, W.R., Thorne, C.R., 2001. Multiple thread flow and channel bifurcation in a braided river: Brahmaputra-Jamuna River, Bangladesh. *Geomorphology* 38, 185–196. [http://dx.doi.org/10.1016/S0169-555X\(00\)00080-5](http://dx.doi.org/10.1016/S0169-555X(00)00080-5).
- Richardson, W.R., Thorne, C.R., Mahmood, S., 1996. Secondary flow and channel changes around a bar in the Brahmaputra River, Bangladesh. In: Ashworth, P.J., Bennet, S.J., Best, J.L., McLelland, S.J. (Eds.), *Coherent Flow Structures in Open Channels*. John Wiley and Sons, Ltd., pp. 519–543.
- Rodrigues, S., Bréhéret, J.G., Macaire, J., Moatar, F., Nistoran, D., Jugé, P., 2006. Flow and sediment dynamics in the vegetated secondary channels of an anabranching river: the Loire River (France). *Sediment. Geol.* 186, 89–109. <http://dx.doi.org/10.1016/j.sedgeo.2005.11.011>.
- Rodrigues, S., Bréhéret, J.G., Macaire, J.J., Greulich, S., Villar, M., 2007. In channel woody vegetation controls on sedimentary processes and the sedimentary record within alluvial environments: a modern example of an anabranch of the River Loire, France. *Sedimentology* 54, 223–242. <http://dx.doi.org/10.1111/j.1365-3091.2006.00832.x>.
- Rodrigues, S., Claude, N., Juge, P., Breheret, J.G., 2012. An opportunity to connect the morphodynamics of alternate bars with their sedimentary products. *Earth Surf. Process. Landf.* 37, 240–248. <http://dx.doi.org/10.1002/esp.2255>.
- Rodrigues, S., Mosselman, E., Claude, N., Wintenberger, C.L., Juge, P., 2015. Alternate bars in a sandy gravel bed river: generation, migration and interactions with superimposed dunes. *Earth Surf. Process. Landf.* 40 (5), 610–628. <http://dx.doi.org/10.1002/esp.3657>.
- Seminara, G., Tubino, M., 1989. Alternate bars and meandering: free, forced and mixed interactions. In: Ikeda, S., Parker, G. (Eds.), *River Meandering*. American Geophysical Union – Water Resources Monographs 12, pp. 267–320 (Washington).
- Sime, L.C., Ferguson, R.I., Church, M., 2007. Estimating shear stress from moving boat acoustic Doppler velocity measurements in a large gravel bed river. *Water Resour. Res.* 43, W03418. <http://dx.doi.org/10.1029/2006WR005069>.
- Simons, D.B., Richardson, E.V., Nordin, C.F., 1965. Bedload equation for ripples and dunes. *US Geological Survey Professional Paper* 462–H.
- Southard, J.B., Boguchwal, L.A., 1990. Bed configuration in steady unidirectional water flows; part 2, synthesis of flume data. *J. Sediment. Res.* 60, 658–679. <http://dx.doi.org/10.1306/212F9241-2B24-11D7-8648000102C1865D>.
- Struiksma, N., Olesen, K.W., Flokstra, C., De Vriend, H.J., 1985. Bed deformation in curved alluvial channels. *J. Hydraul. Res.* 23, 57–79. <http://dx.doi.org/10.1080/00221688509499377>.
- Szupiany, R.N., Amsler, M.L., Best, J.L., Parsons, D.R., 2007. Comparison of fixed- and moving-vessel flow measurements with an aDp in a large river. *J. Hydraul. Eng.* 133, 1299–1308. [http://dx.doi.org/10.1061/\(ASCE\)0733-9429\(2007\)133:12\(1299\)](http://dx.doi.org/10.1061/(ASCE)0733-9429(2007)133:12(1299)).
- Szupiany, R.N., Amsler, M.L., Parsons, D.R., Best, J.L., 2009. Morphology, flow structure, and suspended bed sediment transport at two large braid-bar confluences. *Water Resour. Res.* 45, W05415. <http://dx.doi.org/10.1029/2008WR007428>.
- Ten Brinke, W.B.M., Wilbers, A.W.E., Wesseling, C., 1999. Dune growth, decay and migration rates during a large-magnitude flood at a sand and mixed sand-gravel bed in the Dutch Rhine River System. In: Smith, N.D., Rogers, J. (Eds.), *Fluvial Sedimentology VI: International Association of Sedimentologists Special Publication 28*. Blackwell Publishing Ltd., pp. 15–32.
- Thorne, P.D., Hardcastle, P.J., Soulsby, R.L., 1993. Planform channel evolution of the Brahmaputra River, Bangladesh. In: Best, J.L., Bristow, C.S. (Eds.), *Braided Rivers*. Geological Society Special Publication, London, pp. 257–276.
- Tubino, M., 1991. Growth of alternate bars in unsteady flow. *Water Resour. Res.* 27, 37–52. <http://dx.doi.org/10.1029/90WR01699>.
- Tuijnder, A.P., Ribberink, J.S., Hulscher, S.J.M.H., 2009. An experimental study into the geometry of supply-limited dunes. *Sedimentology* 56, 1713–1727. <http://dx.doi.org/10.1111/j.1365-3091.2009.01054.x>.
- Van Den Berg, J.H., 1987. Bedform migration and bed-load transport in some rivers and tidal environments. *Sedimentology* 34, 681–698. <http://dx.doi.org/10.1111/j.1365-3091.1987.tb00794.x>.
- Van der Mark, C.F., Blom, A., Hulscher, S.J.M.H., 2007. Variability in bedform characteristics using flume and river data. *River, Coast. Estuar. Morphodyn.* 923–930 <http://dx.doi.org/10.1201/NOE0415453639-c117>.
- Van Der Mark, C.F., Blom, A., Hulscher, S.J.M.H., 2008. Quantification of variability in bedform geometry. *J. Geophys. Res.* 113, F03020. <http://dx.doi.org/10.1029/2007JF000940>.
- Van Dijk, W., 2013. *Meandering Rivers: Feedbacks Between Channel Dynamics, Floodplain and Vegetation* (PhD thesis), University of Utrecht (206 pp.).
- Villard, P.V., Church, M., 2003. Dunes and associated sand transport in a tidally influenced sand-bed channel: Fraser River, British Columbia. *Can. J. Earth Sci.* 40, 115–130. <http://dx.doi.org/10.1139/e02-102>.
- Villard, P.V., Church, M., 2005. Bar and dune development during a freshet: Fraser River Estuary, British Columbia, Canada. *Sedimentology* 52, 737–756. <http://dx.doi.org/10.1111/j.1365-3091.2005.00721.x>.
- Whiting, P.J., Dietrich, W.E., 1991. Convective accelerations and boundary shear stress over a channel bar. *Water Resour. Res.* 27, 783–796.
- Wilcock, P.R., 1996. Estimating local bed shear stress from velocity observations. *Water Resour. Res.* 32, 3361. <http://dx.doi.org/10.1029/96WR02277>.
- Wintenberger, C.L., Rodrigues, S., Bréhéret, J.-G., Villar, M., 2015. Fluvial islands: first stage of development from nonmigrating (forced) bars and woody-vegetation interactions. *Geomorphology* 246, 305–320. <http://dx.doi.org/10.1016/j.geomorph.2015.06.026>.
- Wu, F.C., Yeh, T.H., 2005. Forced bars induced by variations of channel width: implications for incipient bifurcation. *J. Geophys. Res.* 110, F02009.
- Wu, F.C., Shao, Y.C., Chen, Y.C., 2011. Quantifying the forcing effect of channel width variations on free bars: morphodynamic modeling based on characteristic dissipative Galerkin scheme. *J. Geophys. Res.* 116, F03023. <http://dx.doi.org/10.1029/2010JF001941>.
- Zolezzi, G., Seminara, G., 2001. Downstream and upstream influence in river meandering: part 1, general theory and application to overdeepening. *J. Fluid Mech.* 438, 183–211. <http://dx.doi.org/10.1017/S002211200100427X>.
- Zolezzi, G., Guala, M., Termini, D., Seminara, G., 2005. Experimental observations of upstream overdeepening. *J. Fluid Mech.* 531, 191–219.
- Zolezzi, G., Bertoldi, W., Tubino, M., 2006. Morphological analysis and prediction of river bifurcations. In: Sambrook Smith, G.H., Best, J.B., Bristow, C.S., Petts, G.E. (Eds.), *Braided Rivers Process, Deposits, Ecology and Management*. Special Publication – International Association of Sedimentologists 36, pp. 233–256.